Performances study of two serial interconnected chemostats with mortality

Manel Dali Youcef, Alain Rapaport, Tewfik Sari

Performances study of two serial interconnected chemostats with mortality

Manel Dali-Youcef [*]   Alain Rapaport[†]   Tewfik Sari[‡]

March 10, 2022

Abstract

In this work, a mathematical model representing two series interconnected chemostats where the mortality of the species is taken into consideration, is studied in detail. The study is carried out with different mortalities of the two tanks. The specificity of this study is the intervention of two types of heterogeneities. There is heterogeneity in relation to the distribution of the total volume in both tanks and heterogeneity in relation to the different mortalities of the two tanks. We study the performance of the serial configuration under two different criteria which consists on the substrate concentration leaving the second tank and the biogas flow rate production. A comparison is made with a single chemostat where the mortality rate is considered to be the same in all tanks, i.e. in the single chemostat and in the interconnected tanks. Conditions depending on the mortality rate, on the parameter defining the distribution of the total volume between the two tanks and on the operating parameters that are the substrate concentration at the entrance of the first tank and the dilution rate, are involved. These conditions allow to have a serial configuration with mortality more efficient than a single chemostat with the same mortality.

Keywords chemostat, gradostat, mortality, bifurcations, global stability, operating diagram, biogas production

AMS Classification 34D20, 34H20, 65K10, 92C75.

Contents

[*]MISTEA, Univ Montpellier, INRAE, Institut Agro, Montpellier, France. Manel.Dali-Youcef@inrae.fr *Present address: Avignon Université, Laboratoire de Mathématiques d'Avignon, Avignon, France.*

[†]MISTEA, Univ Montpellier, INRAE, Institut Agro, Montpellier, France. alain.rapaport@inrae.fr

[‡]ITAP, Univ Montpellier, INRAE, Institut Agro, Montpellier, France; tewfik.sari@inrae.fr

1 Introduction

The mathematical model of the chemostat has received a great attention in the literature for many years (see for instance [16] and literature cited inside). This is probably due to its relative simplicity that can explain and predict quite faithfully the dynamics of real bioprocesses exploiting microbial ecosystems. It is today an important tool for decision making in industrial world, such as for dimensioning bioreactors or designing efficient operating conditions [13, 20]. Several extensions of the original model of the chemostat, considering spatial heterogeneity, have been proposed to better cope reality (see for instance [19]). Lovitt and Wimpenny has proposed the "gradostat" experimental device as a collection of chemostats of same volume interconnected in series [22, 23], which has led to the so-called "gradostat model" representing in a more general framework a gradient of concentrations [36, 39]. The gradostat model has been further generalized as the "general gradostat model" representing more general interconnection graphs with tanks of different volumes [37, 38]. Particular interconnection structures have been investigated and compared for the properties in terms of input-output performances (see for instance [5, 7, 15, 28]). It has been notably shown that a series of reactors instead of a single perfectly mixed one can significantly improve the performances of the bioprocess (in terms of matter conversion) while preserving the same residence time, or equivalently that the same performance can be obtained with a smaller residence time considering several tanks in series instead of a single one [14, 17, 24, 25, 45]. On another hand, it is known that in real processes, various growth conditions can be met and that it could be difficult to setup exactly the same perfect conditions in different reactors. These conditions include toxicity levels of culture media, which means more concretely that the consideration of a bacterial mortality, although often neglected compared to the removal rate, might be non avoidable and could also be variable. To the best of our knowledge, the possible impacts of mortality in the design of series of chemostats has not been yet studied in the literature, which is the purpose of the present work. Its contributions also cover interests in theoretical ecology for a better grasp of the interplay between spatial heterogeneity and mortality in resource-consumers models. Indeed, considering different removal rates in the classical chemostat model or more general ones allows to consider additional mortality terms [21, 29, 33, 43]. However, these mathematical studies have mainly concern analyses of equilibria and stability and not the performances of the system in presence of mortality.

In view of providing clear messages to the practitioners, we investigate how the operating diagram of a series of two interconnected chemosats in series is modified when considering different or identical mortality rates in both tanks. Operating diagrams have proven to be a good synthetic

tool to summarize the possible operating modes, emphasized in [26] for its importance for bioreactors. Indeed, such diagrams are more and more often constructed both in the biological literature [26, 35, 40, 44] and the mathematical literature [1, 2, 4, 9, 10, 11, 12, 18, 30, 31, 32, 34, 41, 42].

Then, we study the performances in terms of conversion ratio and byproduct production (such as biogas). As we shall see, several aspects are not intuitive, which show that the consideration of mortality can significantly modify the favorable operating conditions.

Along the paper, we use the abbreviations LES for locally exponentially stable and GAS for globally exponentially stable in the positive orthant.

The paper is organized as follows. Section 2 includes the introduction of the mathematical model corresponding to the serial configuration of two chemostats with mortality rate. Afterwards, Section 3 focuses on the study of performances of the serial configuration with respect of the output substrate concentration. Then, Section 4 considers the performances of the serial configuration with respect of the biogas production. Next, Section 5 is devoted to illustrations and numerical simulations and a conclusion is given in Section 6. Moreover, we set up the single chemostat with mortality in Appendix A, while Appendix B is devoted to the existence and stability analysis of the steady states of the serial chemostat and Appendix C to its operating diagram. These results are extension of former results, in the case without mortality [7], but that have required to revisit significantly the mathematical proofs. Finally, Appendix D contains technical proofs.

2 Presentation of the model

We consider two serial interconnected chemostats where the total volume V is divided into $V_1 = rV$ and $V_2 = (1-r)V$, with $r \in (0,1)$, as shown in Fig. 1. The substrate and the biomass concentrations in the tank i are respectively denoted S_i and x_i, $i = 1, 2$. The input substrate concentration in the first chemostat is designated S^{in}, the flow rate is constant and is designated by Q. The output substrate concentration is the concentration of substrate in the second tank $S^{out} = S_2$.
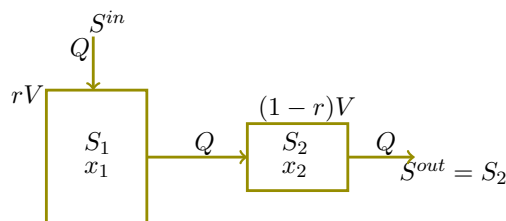
Figure 1: The serial configuration of two chemostats.

The mathematical model is given by the following equations:

$$
\begin{aligned}
\dot{S}_1 &= \frac{D}{r}(S^{in} - S_1) - f(S_1)x_1 \\
\dot{x}_1 &= -\frac{D}{r}x_1 + f(S_1)x_1 - ax_1 \\
\dot{S}_2 &= \frac{D}{1-r}(S_1 - S_2) - f(S_2)x_2 \\
\dot{x}_2 &= \frac{D}{1-r}(x_1 - x_2) + f(S_2)x_2 - ax_2,
\end{aligned}
\tag{1}
$$

where f is the growth function, a is the mortality rate of the biomass and $D = Q/V$ is the dilution rate of the whole structure. The dilution rate of the first tank is $Q/V_1 = D/r$. The dilution rate of the second tank is $Q/V_2 = D/(1-r)$.

Note that these equations are not valid for $r = 0$ and $r = 1$, which correspond to a single chemostat. For sake of completeness, the useful results on the single chemostat are given in Appendix A. The considered growth function satisfies the following properties.

Assumption 1. *The function f is $\mathcal{C}^1$, with $f(0) = 0$ and $f'(S) > 0$ for all $S > 0$.*

3

We define

$$m := \sup_{S>0} f(S), \quad (m \text{ may be } +\infty). \tag{2}$$

As f is increasing then the *break-even concentration* is defined by

$$\lambda(D) := f^{-1}(D) \quad \text{when} \quad 0 \le D < m. \tag{3}$$

The particular case without mortality of the biomass ($a = 0$) is studied in [7]. The results on the existence and stability of steady states of system (1) are very similar to the case without mortality. The details are given in Appendix B. The system can have up to three steady states:

- The washout steady state $E_0 = (S^{in}, 0, S^{in}, 0)$.

- The steady state $E_1 = (S^{in}, 0, \overline{S}_2, \overline{x}_2)$ of washout in the first chemostat but not in the second one.

- The steady state $E_2 = (S_1^*, x_1^*, S_2^*, x_2^*)$ of persistence of the species in both chemostats.

As in the case without mortality, see Table 3 in the Appendix, for any operating condition (S^{in}, D), one and only one of the steady-states E_0, E_1 and E_2, is stable. It is then globally asymptotically stable (GAS).

The operating diagram of the system is described in Appendix C. The operating diagram has as coordinates the input substrate concentration S^{in} and the dilution rate D, and shows how the solutions of the system behave for different values of these two parameters. The regions constituting the operating diagram correspond to different qualitative asymptotic behaviors. The operating diagram of system (1) is depicted in Fig. 2.

The aim of this work is to establish a comparison of the performance of the serial configuration with ones of the single chemostat. In the following, we compare both structures according to two different criteria; the output substrate concentration and the biogas flow rate.

3   Output substrate concentration

We assume that the serial configuration is functioning at a stable steady state. The output substrate concentration at steady state depends on the parameters D, S^{in} and r. It is denoted $S_r^{out}(S^{in}, D)$.

Proposition 1. *Assume that Assumption 1 is satisfied. The output substrate concentration at steady state of system* (1) *is given by*

$$S_r^{out}(S^{in}, D) = \begin{cases} S^{in} & if & S^{in} \le \min\left(\lambda\left(\frac{D}{1-r} + a\right), \lambda\left(\frac{D}{r} + a\right)\right) \\ \overline{S}_2 & if & \lambda\left(\frac{D}{1-r} + a\right) \le S^{in} \le \lambda\left(\frac{D}{r} + a\right) \\ S_2^* & if & S^{in} > \lambda\left(\frac{D}{r} + a\right) \end{cases} \tag{4}$$

where $\overline{S}_2 = \lambda\left(\frac{D}{1-r} + a\right)$ and S_2^* is the unique solution of equation $h(S_2) = f(S_2)$. In this equation, the function h is defined by:

$$h(S_2) = \frac{D + (1-r)a}{1-r} \frac{S_1^* - S_2}{b - S_2}, \tag{5}$$

where $S_1^* = \lambda\left(\frac{D}{r} + a\right)$ and $b = \frac{D(S^{in} - S_1^*)}{D + ra} + S_1^*$.

Proof. The output substrate concentration at steady state of system (1) is equal to S^{in}, if E_0 is the GAS steady state. It is equal to $\overline{S}_2$ if E_1 is the GAS steady state and to S_2^* if E_2 is GAS. According to Theorem 3 in the Appendix, E_0 is GAS if and only if

$$D \ge \max(r, 1 - r)(f(S^{in}) - a),$$

4

which is equivalent to

$$S^{in} \leq \min\left(\lambda\left(\tfrac{D}{1-r}+a\right), \lambda\left(\tfrac{D}{r}+a\right)\right).$$

On the other hand, using Theorem 3, $\overline{S}_2$ depends on D and r and we have $\overline{S}_2 = \lambda\left(\tfrac{D}{1-r}+a\right)$. E_1 is GAS if and only if

$$r(f(S^{in})-a) \leq D \leq (1-r)(f(S^{in})-a),$$

which is equivalent to

$$\lambda\left(\tfrac{D}{1-r}+a\right) \leq S^{in} \leq \lambda\left(\tfrac{D}{r}+a\right).$$

Finally, using Theorem 3, we know that S_2^* depends on parameters S^{in}, D, r. It is the unique solution of equation $h(S_2) = f(S_2)$, where h is defined by (5). On the other hand E_2 is GAS if and only if the condition $D < r(f(S^{in})-a)$ is satisfied, which is equivalent to the condition $S^{in} > \lambda\left(\tfrac{D}{r}+a\right)$. □

Although $S_r^{out}(S^{in}, D)$ is defined only for $0 < r < 1$, we can extend it, by continuity, for $r = 0$ and $r = 1$ by

$$S_0^{out}(S^{in}, D) = S_1^{out}(S^{in}, D) = S^{out}(S^{in}, D). \tag{6}$$

where $S^{out}(S^{in}, D)$, which is the output substrate concentration of the single chemostat, is given by

$$S^{out}(S^{in}, D) = \begin{cases} S^{in} & \text{if} \quad S^{in} \leq \lambda(D+a), \\ \lambda(D+a) & \text{if} \quad S^{in} > \lambda(D+a). \end{cases} \tag{7}$$

For more information on $S^{out}(S^{in}, D)$, see Appendix A.

The proof of (6), comes from the following remarks. First, we have $\overline{S}_2(D, 0) = \lambda(D+a)$ and second, according to Lemma 9 in the Appendix, we can extend $S_2^*(S^{in}, D, r)$, by continuity, to $r = 1$, by

$$S_2^*(S^{in}, D, 1) = \lambda(D+a).$$

Our aim in this section is to compare S_r^{out} defined by (4) and (6) and S^{out} defined by (7).

3.1 The serial configuration can be more efficient than the single chemostat

We fix r and we describe the set of operating conditions (S^{in}, D) for which

$$S_r^{out}(S^{in}, D) < S^{out}(S^{in}, D), \tag{8}$$

that is to say, the serial configuration with volumes rV and $(1-r)V$, is more efficient than the single chemostat of volume V. For $r \in (0, 1)$, let $g_r : [0, r(m-a)) \mapsto \mathbb{R}$ defined by

$$g_r(D) := \lambda\left(\tfrac{D}{r}+a\right) + \tfrac{r(D+ar)}{(1-r)(D+a)}\left(\lambda\left(\tfrac{D}{r}+a\right) - \lambda(D+a)\right). \tag{9}$$

Lemma 1. *For $r \in (0, 1)$ we have $g_r(D) > \lambda\left(\tfrac{D}{r}+a\right)$.*

Proof. As $0 < r < 1$ and λ is an increasing function then, we have $\lambda(D/r+a) > \lambda(D+a)$. Using (9), we have $g_r(D) > \lambda(D/r+a)$. □
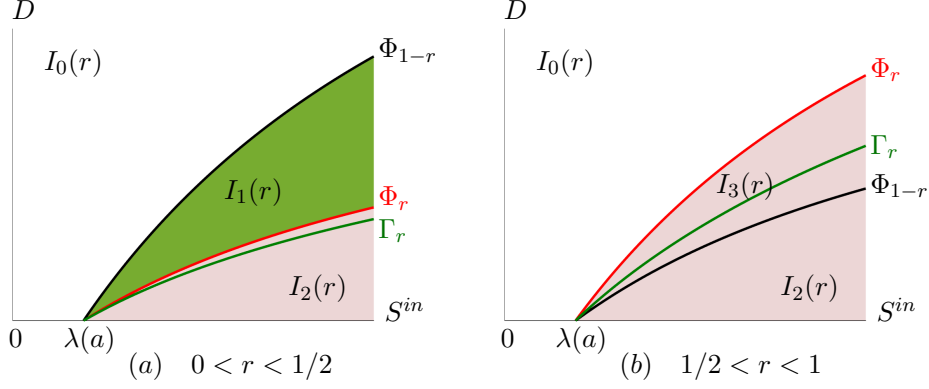
Figure 2: The operating diagram of of system (1) and the curve Γ_r defined by (14).

Theorem 1. *Assume that Assumption 1 is satisfied. For any $r \in (0,1)$, we have*

$$S_r^{out}(S^{in}, D) = S^{out}(S^{in}, D) \Longleftrightarrow S^{in} = g_r(D).$$

Moreover,

$$S_r^{out}(S^{in}, D) < S^{out}(S^{in}, D) \Longleftrightarrow S^{in} > g_r(D).$$

Proof. Recall that $S_2^*(S^{in}, D, r)$ is the unique solution of equation $f(S_2) = h(S_2)$ with h defined by (5). Let us first prove that

$$S_2^*(S^{in}, D, r) < \lambda(D + a) \Longleftrightarrow S^{in} > g_r(D). \tag{10}$$

Since f is increasing, see Assumption 1, and h is decreasing, see Lemma 8 in the Appendix, then the condition $S_2^*(S^{in}, D, r) < \lambda(D + a)$ is equivalent to the condition $h(\lambda(D + a)) < f(\lambda(D + a)) = D + a$. Using (5), a straightforward computation shows that the condition $h(\lambda(D + a)) < D + a$ is equivalent to $S^{in} > g_r(D)$, where g_r is defined by (9). This proves (10). Let us go now to the proof of the theorem. Assume that $S^{in} > g_r(D)$. Using Lemma 1, we have

$$S^{in} > \lambda(D/r + a) > \lambda(D + a).$$

Using (4) and (7), we have

$$\begin{aligned} S_r^{out}(S^{in}, D) &= S_2^*(S^{in}, D, r), \\ S^{out}(S^{in}, D) &= \lambda(D + a). \end{aligned} \tag{11}$$

From (10), we have $S_r^{out}(S^{in}, D) < S^{out}(S^{in}, D)$. Hence, we proved the following implication

$$S^{in} > g_r(D) \Longrightarrow S_r^{out}(S^{in}, D) < S^{out}(S^{in}, D). \tag{12}$$

Assume now that $S^{in} \leq g_r(D)$. When $r < 1/2$, three cases must be distinguished. First, if

$$\lambda(D + a) < \lambda\left(\tfrac{D}{r} + a\right) < S^{in} \leq g_r(D),$$

then, by (4) and (7), we obtain (11). Hence, using (10), we have $S_r^{out}(S^{in}, D) \geq S^{out}(S^{in}, D)$. Secondly, if

$$\lambda(D + a) < \lambda\left(\tfrac{D}{1-r} + a\right) \leq S^{in} \leq \lambda\left(\tfrac{D}{r} + a\right),$$

then, by (4) and (7), we have

$$\begin{aligned} S_r^{out}(S^{in}, D) &= \lambda\left(\tfrac{D}{1-r} + a\right), \\ S^{out}(S^{in}, D) &= \lambda(D + a). \end{aligned}$$

6

Therefore, we have $S_r^{out}(S^{in}, D) > S^{out}(S^{in}, D)$. Finally, if $S^{in} \leq \lambda(D + a)$, then

$$S_r^{out}(S^{in}, D) = S^{out}(S^{in}, D) = S^{in}.$$

When $r \geq 1/2$, the proof is similar, excepted that we must distinguish only two cases, $\lambda(D + a) < S^{in} \leq \lambda(D/r + a)$ and $S^{in} \leq \lambda(D + a)$. Hence, we have proved the reciprocal implication of (12). This completes the proof of second equivalence in the theorem.

The same calculations show the equivalence if inequalities are replaced by equalities. $\qquad\square$

Theorem 1 asserts that the serial configuration is more efficient than the single chemostat if and only if $S^{in} > g_r(D)$. Let us illustrate this result in the operating diagram of system (1). Consider the curve of equation

$$\Phi_r = \left\{ (S^{in}, D) : S^{in} = \lambda(D/r + a) \right\}. \tag{13}$$

According to the results given in Appendix C, the curves Φ_r and Φ_{1-r} defined by (13) separate the operating plane (S^{in}, D) in four regions in which the system has different asymptotic behaviour, see Table 3. To put it simply, in the $I_0(r)$ region, E_0 is GAS, in $I_1(r)$, E_1 is GAS, and in $I_2(r) \cap I_3(r)$, E_3 is GAS, see Fig. 2. This figure also shows the plot of the curve Γ_r, defined by

$$\Gamma_r := \left\{ (S^{in}, D) : S^{in} = g_r(D) \right\}. \tag{14}$$

Using Lemma 1, we see that for all $r \in (0, 1)$, the curve Γ_r is always at right of the curve Φ_r. According to Theorem 1, the output substrate concentration of the serial configuration is smaller than the one of the single chemostat, if and only if (S^{in}, D) is at right of the curve Γ_r depicted in Fig. 2.

3.2 The output substrate concentration as a function of the volume fraction r

In this section we assume that (S^{in}, D) is fixed and we look at the values of r for which (8) holds. More precisely we are going to describe the function

$$r \mapsto S_r^{out}(S^{in}, D). \tag{15}$$

Proposition 2. *Assume that Assumption 1 is satisfied. Let $D > 0$, $S^{in} > \lambda(a)$. We denote $r_0 = D/(f(S^{in}) - a)$.*

1. *If $S^{in} \leq \lambda(D + a)$, then for any $r \in [0, 1]$, one has $S_r^{out}(S^{in}, D) = S^{out}(S^{in}, D) = S^{in}$.*

2. *If $\lambda(D + a) < S^{in} < \lambda(2D + a)$, then $1/2 < r_0 < 1$ and one has*

$$S_r^{out}(S^{in}, D) = \begin{cases} \overline{S}_2 & if \quad 0 \leq r \leq 1 - r_0 \\ S^{in} & if \quad 1 - r_0 \leq r \leq r_0 \\ S_2^* & if \quad r_0 \leq r \leq 1. \end{cases} \tag{16}$$

3. *If $\lambda(2D + a) \leq S^{in}$, then $0 < r_0 \leq 1/2$ and one has*

$$S_r^{out}(S^{in}, D) = \begin{cases} \overline{S}_2 & if \quad 0 \leq r \leq r_0 \\ S_2^* & if \quad r_0 \leq r \leq 1. \end{cases} \tag{17}$$

Here $\overline{S}_2 = \lambda\left(\frac{D}{1-r} + a\right)$ and $S_2^* = S_2^*(S^{in}, D, r)$ is the unique solution of equation $f(S_2) = h(S_2)$, where h is defined by (5).

Proof. If $S^{in} \leq \lambda(D + a)$, then, for all $r \in (0, 1)$, one has

$$S^{in} \leq \lambda(D + a) \leq \min\left\{\lambda\left(\frac{D}{1-r} + a\right), \lambda\left(\frac{D}{r} + a\right)\right\}.$$

Then, according to (4), one has $S_r^{out}(S^{in}, D) = S^{in}$. This proves item 1 of the proposition.

Let $r_0 = D/(f(S^{in}) - a)$, i.e. $S^{in} = \lambda(D/r_0 + a)$.

If $\lambda(D + a) < S^{in} < \lambda(2D + a)$, then $r_0 \in (1/2, 1)$, so that $1 - r_0 < r_0$. The interval $[0, 1]$ is subdivided into three sub-intervals. Firstly, if $0 \leq r \leq 1 - r_0 < r_0$, then $r < r_0 \leq 1 - r$, so that

$$\lambda\left(\frac{D}{1-r} + a\right) \leq S^{in} = \lambda\left(\frac{D}{r_0} + a\right) < \lambda\left(\frac{D}{r} + a\right).$$

Hence, according to (4), one has

$$S_r^{out}(S^{in}, D) = \lambda\left(\frac{D}{1-r} + a\right).$$

Secondly, if $1 - r_0 \leq r \leq r_0$, then $r_0 \geq \max\{r, 1 - r\}$, so that

$$S^{in} = \lambda\left(\frac{D}{r_0} + a\right) \leq \min\left\{\lambda\left(\frac{D}{1-r} + a\right), \lambda\left(\frac{D}{r} + a\right)\right\}.$$

Hence, according to (4), one has $S_r^{out}(S^{in}, D) = S^{in}$. Finally, if $r_0 < r \leq 1$, then one has

$$S^{in} = \lambda\left(\frac{D}{r_0} + a\right) > \lambda\left(\frac{D}{r} + a\right).$$

Hence, according to (4), one has

$$S_r^{out}(S^{in}, D) = S_2^*(S^{in}, D, r).$$

This proves item 2 of the proposition.

If $\lambda(2D + a) \leq S^{in}$, then $r_0 \in (0, 1/2]$. Therefore, $r_0 \leq 1 - r_0$. The proof of item 3 of the proposition is the same as the proof of item 2 excepted that now, the interval $[0, 1]$ is subdivided now into two sub-intervals $[0, r_0]$ and $[r_0, 1]$, so that the interval for which $S_r^{out}(S^{in}, D) = S^{in}$ is empty. $\qquad\square$
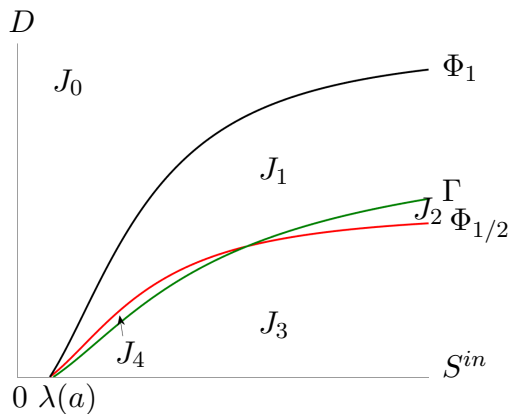
Figure 3: In each region, the map $r \mapsto S_r^{out}(S^{in}, D)$ for fixed (S^{in}, D) has a different behavior.

We want to determine the values $r \in (0, 1)$ for which the condition (8) is satisfied. We need the following Assumption that is satisfied by any concave growth function but also by non concave growth functions, satisfying additional conditions, see Section 3.4.

Assumption 2. *For every $D \in [0, m - a)$, the function $r \in (D/(m - a), 1) \mapsto g_r(D) \in \mathbb{R}$ is decreasing.*

Let $D < m - a$. Using $g_r(D) > \lambda(D/r + a)$, we have

$$\lim_{r \to D/(m-a)} g_r(D) > \lim_{r \to D/(m-a)} \lambda(D/r + a) = +\infty.$$

On the other hand, using L'Hôpital's rule, we have

$$\lim_{r \to 1} g_r(D) = g(D). \tag{18}$$

where $g : [0, m - a) \to \mathbb{R}^+$ is defined by

$$g(D) = \lambda(D + a) + D\lambda'(D + a). \tag{19}$$

Therefore, from Assumption 2, the function $r \mapsto g_r(D)$ is decreasing from $(D/(m-a), 1)$ to $(g(D), +\infty)$. Hence, it admits an inverse function

$$S^{in} \in (g(D), +\infty) \mapsto r_1(S^{in}, D) \in (D/(m-a), 1).$$

We use the notation $r_1(\cdot, D)$ to recall the dependence of the inverse function in D. For all $D \in (0, m - a)$, $r \in (D/(m-a), 1)$ and $S^{in} > g(D)$, we have

$$r = r_1(S^{in}, D) \iff S^{in} = g_r(D), \tag{20}$$
$$r > r_1(S^{in}, D) \iff S^{in} > g_r(D). \tag{21}$$

Theorem 2. *Assume that Assumptions 1 and 2 are satisfied. Let g defined by* (19).

- *If $S^{in} \leq g(D)$ then for any $r \in (0, 1)$, we have $S_r^{out}(S^{in}, D) > S^{out}(S^{in}, D)$. In addition, for $r = 0$ and $r = 1$ we have $S_r^{out}(S^{in}, D) = S^{out}(S^{in}, D)$.*

- *If $S^{in} > g(D)$ then $S_r^{out}(S^{in}, D) < S^{out}(S^{in}, D)$ if and only if $r_1(S^{in}, D) < r < 1$, with $r_1(S^{in}, D)$, defined by* (20). *In addition, for $r = 0$, $r = r_1(S^{in}, D)$ and $r = 1$, we have $S_r^{out}(S^{in}, D) = S^{out}(S^{in}, D)$.*

Proof. The function $r \mapsto g_r(D)$ is decreasing and tends to $g(D)$ as r tends to 1, as shown by (18). Thus, for all $r \in (0, 1)$, we have $g(D) < g_r(D)$. If $S^{in} \leq g(D)$, then $S^{in} < g_r(D)$. According to Theorem 1, for all $r \in (0, 1)$, we have $S_r^{out}(S^{in}, D) > S^{out}(S^{in}, D)$.

Let $S^{in} > g(D)$. Let $r_1 = r_1(S^{in}, D)$. According to (21), for all $r > r_1$, we have $S^{in} > g_r(D)$. Thus, according to Theorem 1, we have $S_r^{out}(S^{in}, D) < S^{out}(S^{in}, D)$.

The equality $S_r^{out}(S^{in}, D) = S^{out}(S^{in}, D)$ is verified for the $r = 0$ and $r = 1$, see (6). In addition, we have $S^{in} = g_{r_1}(D)$, see (20). Hence, according to Theorem 1, we have $S_{r_1}^{out}(S^{in}, D) = S^{out}(S^{in}, D)$. $\qquad\square$

Let us now describe the subsets of the operational space (S^{in}, D) for which the behaviour described in the three cases of Proposition 2 occurs. For a complete description we will also distinguish the sub-cases for which there exists $r_1 = r_1(S^{in}, D)$ such that, for $r_1 < r < 1$, (8) is satisfied, as shown in Theorem 2. Consider the curves Φ_1 and $\Phi_{1/2}$, defined by (13), and the curve Γ defined by

$$\Gamma := \{(S^{in}, D) : S^{in} = g(D)\}, \tag{22}$$

These three curves intersect at $(\lambda(a), 0)$ and, using the inequality $g(D) > \lambda(D + a)$, which is satisfeied for all $D > 0$, one deduces that Γ is at the right of Φ_1. Therefore, the curves Φ_1, $\Phi_{1/2}$ and Γ separate the set of operating parameters (S^{in}, D) into the following four subsets, see Fig. 3.
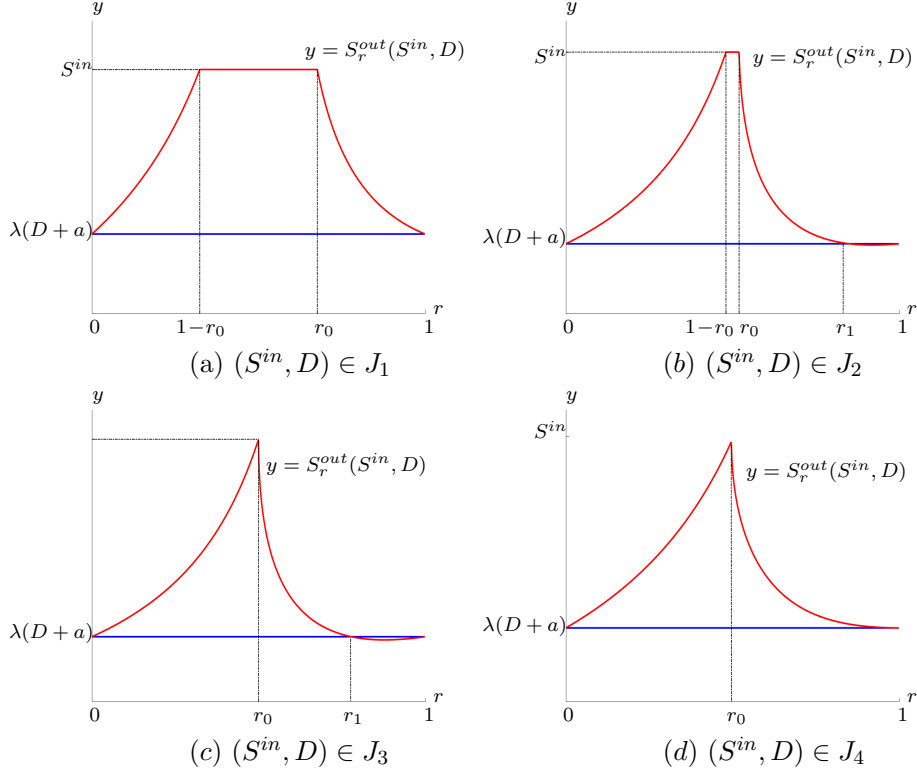
Figure 4: For S^{in} and D fixed, the output substrate concentration of the serial configuration, in red, compared to that of the single chemostat, in blue; $r_1(S^{in}, D)$ is defined by (20), $r_0 = D/(f(S^{in}) - a)$ and J_1, J_2, J_3, J_4 are depicted in Fig. 3.

$$
\begin{aligned}
J_0 &= \left\{ (S^{in}, D) : S^{in} \leq \lambda(D + a) \right\}, \\
J_1 &= \left\{ (S^{in}, D) : \lambda(D + a) < S^{in} \leq \min\{g(D), \lambda(2D + a)\} \right\}, \\
J_2 &= \left\{ (S^{in}, D) : g(D) < S^{in} < \lambda(2D + a) \right\}, \\
J_3 &= \left\{ (S^{in}, D) : \max\{g(D), \lambda(2D + a)\} \leq S^{in} \right\}, \\
J_4 &= \left\{ (S^{in}, D) : \lambda(2D + a) < S^{in} < g(D) \right\}.
\end{aligned}
\tag{23}
$$

Combining the results of Proposition 2 and Theorem 2, we find that the function $r \mapsto S_r^{out}(S^{in}, D)$ is as in Fig. 4. In the following we will comment on this figure.

- If $(S^{in}, D) \in J_1$, then when $S^{in} < \lambda(2D + a)$, $S_r^{out}(S^{in}, D)$ is given by (16) and when $S^{in} = \lambda(2D + a)$, $S_r^{out}(S^{in}, D)$ is given by (17). In addition, for all $r \in (0, 1)$, $S_r^{out}(S^{in}, D) > S^{out}(S^{in}, D)$. The equality is fulfilled for $r = 0$ and $r = 1$, see Fig. 4(a).

- If $(S^{in}, D) \in J_2$, then $S_r^{out}(S^{in}, D)$ is given by (16) and $S_r^{out}(S^{in}, D) < S^{out}(S^{in}, D)$ if and only if $r \in (r_1(S^{in}, D), 1)$, where $r_1(S^{in}, D)$ is defined by (20). The equality is fulfilled for $r = 0$, $r = r_1(S^{in}, D)$ and $r = 1$, see Fig. 4(b).

- If $(S^{in}, D) \in J_3$ then $S_r^{out}(S^{in}, D)$ is given by (17) and $S_r^{out}(S^{in}, D) < S^{out}(S^{in}, D)$ if and only if $S^{in} > g(D)$ and $r \in (r_1(S^{in}, D), 1)$ where $r = r_1(S^{in}, D)$ is defined by (20). The equality is fulfilled for $r = 0$, $r = r_1(S^{in}, D)$ and $r = 1$, see Fig. 4(c).

- If $(S^{in}, D) \in J_4$ then $S_r^{out}(S^{in}, D)$ is given by (17) and for all $r \in (0, 1)$, $S_r^{out}(S^{in}, D) > S^{out}(S^{in}, D)$. The equality is fulfilled for $r = 0$ and $r = 1$, see Fig. 4(d).

Note that if $(S^{in}, D) \in J_0$, then case 1 of Proposition 2 occurs. One remarks that the lowest value of the red curve, corresponding to the lowest output substrate concentration of the serial

configuration, is obtained for $(S^{in}, D) \in J_2 \cap J_3$ and $r > r_1(S^{in}, D)$. This lowest concentration is obtained with the best possible serial configuration.

Figures 2, 3 and 4 are made without graduations on the axes because they represent general situations where the growth function is only assumed to verify our hypotheses. It should be noticed that regions J_0, J_1 and J_3 always exist and are connected. However, regions the J_2 and J_4 do not always exist or are necessarily connected. This depends on the number of points of intersection between curves $\Phi_{1/2}$ and Γ. For a linear growth rate, $\Phi_{1/2} = \Gamma$ and hence, regions J_2 and J_4 do not exist, see Fig. 7(a). For a Monod growth function, curves $\Phi_{1/2}$ and Γ intersect only at point $(\lambda(a), 0)$ and hence, region J_3 always exist and is connected but region J_3 does not exist, see Fig. 8(a). For a Hill growth function, curves $\Phi_{1/2}$ and Γ always intersect at $(\lambda(a), 0)$ and also at a unique positive point, Lemma 6. Hence, regions J_2 and J_4 both exist and are connected, see Fig. 9(a,b,c).

3.3 The output substrate concentration as a function of the dilution rate

In this section we assume that S^{in} and r are fixed and we look at the values of the dilution rate D for which (8) holds, i.e. the serial configuration, is more efficient than the single chemostat. More precisely we are going to describe the function

$$D \mapsto S_r^{out}(S^{in}, D). \tag{24}$$

We want to determine the subset of values of D for which the condition (8) is satisfied. We need the following Assumption that is satisfied by any concave growth function, but also by non concave growth functions, satisfying additional conditions, see Section 3.4.

Assumption 3. *For every $r \in (0, 1)$, the function $D \in [0, r(m - a)) \mapsto g_r(D) \in \mathbb{R}$ is increasing.*

Using $g_r(D) > \lambda(D/r + a)$, we have

$$\lim_{D \to r(m-a)} g_r(D) > \lim_{D \to r(m-a)} \lambda(D/r + a) = +\infty.$$

From Assumption 3, the function $D \mapsto g_r(D)$ is increasing from $[0, r(m - a))$ to $[g_r(0) = \lambda(a), +\infty)$. Hence, its admits an inverse function

$$S^{in} \in (\lambda(a), +\infty) \mapsto D_r(S^{in}) \in [0, r(m - a)).$$

For all $r \in (0, 1)$, $S^{in} \geq \lambda(a)$ and $D \in [0, r(m - a))$, we have

$$D = D_r(S^{in}) \iff S^{in} = g_r(D), \tag{25}$$

$$D < D_r(S^{in}) \iff S^{in} > g_r(D). \tag{26}$$

Proposition 3. *Assume that Assumptions 1 and 3 are satisfied. We have*

$$S_r^{out}(S^{in}, D) < S^{out}(S^{in}, D) \iff 0 < D < D_r(S^{in}),$$

where $D_r(S^{in})$ is defined by (25).

Proof. Let $r \in (0, 1)$. According to (26), if $D < D_r(S^{in})$, then $S^{in} > g_r(D)$. Consequently, according to Theorem 1, we have $S_r^{out}(S^{in}, D) < S^{out}(S^{in}, D)$. $\qquad\square$

3.4 How to check Assumptions 2 and 3

In this section we give sufficient conditions for Assumption 2 and 3 to be satisfied. These conditions will be useful for the applications given in Section 5. For this purpose we consider the function γ defined by

$$\gamma(r, D) = g_r(D), \tag{27}$$

defined on
$$\text{dom}(\gamma) = \{(r, D) : 0 < r < 1, 0 < D/r + a < m\},$$
which consists simply in considering $g_r(D)$, given by (9), as a function of both variables r and D. If

$$\frac{\partial \gamma}{\partial r}(r, D) < 0 \text{ for all } (r, D) \in \text{dom}(\gamma),$$

then Assumption 2 is satisfied. Similarly, if

$$\frac{\partial \gamma}{\partial D}(r, D) > 0 \text{ for all } (r, D) \in \text{dom}(\gamma),$$

then Assumption 3 is satisfied. The following Lemmas give sufficient conditions, for partial derivatives of γ to have their signs as indicated above.

Lemma 2. *For $D \in (0, m - a)$, let l_D be defined on $\text{dom}(l_D) = (D/(m - a), 1]$ by $l_D(r) = \lambda(D/r + a)$.*

a *Assume that for $D \in (0, m - a)$ and $r \in \text{dom}(l_D)$ we have*

$$l_D(1) > l_D(r) + (1 - r)l'_D(r) \tag{28}$$

then, for all $(r, D) \in \text{dom}(\gamma)$, we have $\frac{\partial \gamma}{\partial r}(r, D) < 0$.

b *If, for $D \in (0, m - a)$, l_D is strictly convex on $\text{dom}(l_D)$, then the condition (28) is satisfied.*

c *If f is twice derivable, then l_D is twice derivable and the following conditions are equivalent*

    1 *For $D \in (0, m - a)$ and $r \in \text{dom}(l_D)$, $l''_D(r) > 0$.*
    2 *For $S > \lambda(a)$, $(f(S) - a)f''(S) < 2 (f'(S))^2$.*

Proof. Notice first that $\gamma(r, D)$ can be written as follows

$$
\begin{aligned}
\gamma(r, D) \quad &= g_r(D) = \lambda(D + a) + \\
&\left(\frac{1}{1-r} - \frac{ra}{D+a}\right) \left(\lambda\left(\frac{D}{r} + a\right) - \lambda(D + a)\right).
\end{aligned}
\tag{29}
$$

Using the definition of l_D, $\gamma(r, D)$ is given then by

$$\gamma(r, D) = l_D(1) + \left(\frac{1}{1-r} - \frac{ra}{D+a}\right)(l_D(r) - l_D(1)).$$

The partial derivative, with respect to r of γ is given then by

$$
\begin{aligned}
\frac{\partial \gamma}{\partial r}(r, D) &= \frac{a(1-2r)}{D+a}l'_D(r) + \\
&\left(\frac{1}{(1-r)^2} - \frac{a}{D+a}\right)(l_D(r) - l_D(1) + (1 - r)l'_D(r)).
\end{aligned}
\tag{30}
$$

Notice that $\frac{1}{(1-r)^2} - \frac{a}{D+a} > 0$ for all $r \in (0, 1)$. From $l'_D(r) = -\frac{D}{r^2}\lambda'\left(\frac{D}{r} + a\right)$, it is deduced that $l'_D(r) < 0$. Therefore, if the condition (28) is satisfied, and, in addition $0 < r \leq 1/2$, then, from (30), it is deduced that $\frac{\partial \gamma}{\partial r}(r, D) < 0$.
In the case $r \in (1/2, 1)$, we use the following expression of $\gamma(r, D)$ which is deduced from (29):

$$\gamma(r, D) = l_D(1) + B(r)\frac{l_D(r) - l_D(1)}{1 - r},$$

where $B(r) = \frac{D + a - ar(1 - r)}{D + a}$. Straightforward computation show that

$$
\begin{aligned}
\frac{\partial \gamma}{\partial r}(r, D) &= \\
&\frac{D + ar(2 - r)}{(D+a)(1-r)^2}(l_D(r) - l_D(1) + (1 - r)C(r)l'_D(r)),
\end{aligned}
\tag{31}
$$

where $C(r) = \frac{D+a-ar(1-r)}{D+ar(2-r)}$. We have

$$C'(r) = \frac{a}{(D+ar(2-r))^2} \left(ar^2 + 2(a+2D)r - 3D - 2a \right).$$

Thus $C'(r) = 0$ for

$$r = r^* := \frac{1}{a} \left(\sqrt{3a^2 + 7aD + 4D^2} - a - 2D \right) \in (1/2, 1)$$

and $(r - r^*)C'(r) > 0$ for $r \in (1/2, 1)$, $r \neq r^*$. Hence, from $C(1/2) = C(1) = 1$, we have $0 < C(r) < 1$ for all $r \in (1/2, 1)$. Now, if we assume that (28) is satisfied, for $1/2 < r < 1$ we have

$$l_D(1) > l_D(r) + (1-r)l'_D(r) > l_D(r) + (1-r)C(r)l'_D(r).$$

Hence, from (31), it is deduced that $\frac{\partial \gamma}{\partial r}(r, D) < 0$. This proves part a of the lemma.

Moreover, if l_D is strictly convex on $\mathrm{dom}(l_D)$ then for all s and r in $(D/(m-a), 1]$, if $s \neq r$, then

$$l_D(s) > l_D(r) + (s-r)l'_D(r).$$

Taking $s = 1$ and $r \in \mathrm{dom}(l_D)$ one obtains the condition (28). This proves part b of the lemma. Assume now that f, and hence l_D, are twice derivable. Using

$$\lambda'(D) = \frac{1}{f'(\lambda(D))}, \quad \lambda''(D) = -\frac{f''(\lambda(D))}{(f'(\lambda(D)))^3}, \tag{32}$$

we can write

$$\begin{aligned}
l''_D(r) &= \frac{2D}{r^3}\lambda'\left(\frac{D}{r}+a\right) + \frac{D^2}{r^4}\lambda''\left(\frac{D}{r}+a\right) \\
&= \frac{D\left(2\left(f'\left(\lambda\left(\frac{D}{r}+a\right)\right)\right)^2 - \frac{D}{r}f''\left(\lambda\left(\frac{D}{r}+a\right)\right)\right)}{r^3\left(f'\left(\lambda\left(\frac{D}{r}+a\right)\right)\right)^3}.
\end{aligned}$$

Therefore, the condition 1 in item c in the lemma is equivalent to the following condition: For all $D \in (0, m-a)$ and $r \in (D/(m-a), 1]$, we have

$$\frac{D}{r}f''\left(\lambda\left(\frac{D}{r}+a\right)\right) < 2f'\left(\lambda\left(\frac{D}{r}+a\right)\right)^2. \tag{33}$$

Using the notation $S = \lambda\left(\frac{D}{r}+a\right)$, which is the same as $D/r = f(S) - a$, the condition (33) is equivalent to : For all $S > 0$, $(f(S) - a)f''(S) < 2\left(f'(S)\right)^2$, which is the condition 2 in c in the lemma. $\qquad \square$

Lemma 3. *Assume that*

$$f'\left(\lambda\left(\frac{D}{r}+a\right)\right) \leq \frac{1}{r}f'\left(\lambda(D+a)\right). \tag{34}$$

Then, $\frac{\partial \gamma}{\partial D}(r, D) > 0$. Hence Assumption 3 is satisfied. If f' is decreasing, then the condition (34) is satisfied.

Proof. From (29) we deduce that

$$\begin{aligned}
\frac{\partial \gamma}{\partial D}(r, D) &= \lambda'(D+a) + \frac{ra}{(D+a)^2}\left(\lambda\left(\frac{D}{r}+a\right) - \lambda(D+a)\right) \\
&\quad + \left(\frac{1}{1-r} - \frac{ra}{D+a}\right)\left(\frac{1}{r}\lambda'\left(\frac{D}{r}+a\right) - \lambda'(D+a)\right).
\end{aligned}$$

Notice that $\frac{1}{1-r} - \frac{ra}{D+a} > 0$, $\lambda'(D+a) > 0$ and $\lambda\left(\frac{D}{r}+a\right) > \lambda(D+a)$. Therefore the condition

$$\frac{1}{r}\lambda'\left(\frac{D}{r}+a\right) - \lambda'(D+a) \geq 0$$

is sufficient to have $\frac{\partial \gamma}{\partial D}(r, D) > 0$. Using (32), this condition is equivalent to (34). Note that if f' is decreasing, then this condition is satisfied. Indeed, we have

$$f'\left(\lambda\left(\frac{D}{r}+a\right)\right) \leq f'\left(\lambda(D+a)\right) \leq \frac{1}{r}f'\left(\lambda(D+a)\right),$$

which is the condition (34). $\qquad \square$

Remark 1. *Notice that:*

i *The condition 2 in part c of Lemma 2 is equivalent to the condition*

$$\text{For all } S > \lambda(a), \frac{d^2}{dS^2}\left(\frac{1}{f(S)-a}\right) > 0. \tag{35}$$

Therefore, if f satisfies the condition (35), then it verifies Assumption 2.

ii *If the increasing growth function f is twice derivable and satisfies $f''(S) \le 0$ for all $S > 0$, then the condition b in Lemma 2 and the condition (34) in Lemma 3 are satisfied. Thus, Assumptions 2 and 3 are satisfied and our results apply for any concave growth function.*

iii *Assume that the increasing growth function f is twice derivable and there exists $\hat{S} \in (0, +\infty)$ such that f'' is nonnegative on $(0, \hat{S})$ and nonpositive on $(\hat{S}, +\infty)$. If moreover the condition 2 in part c of Lemma 2 is verified for $a = 0$, then this condition is also verified for any $a > 0$ and $S \in (\lambda(a), \hat{S})$. Therefore, if $(1/f)'' > 0$ on $(0, \hat{S})$ then Assumption 2 is satisfied.*

We will see in Section 5, how to use Remark 1 and Lemmas 2 and 3 to show that a linear growth function, a Monod function and a Hill function satisfy Assumptions 2 and 3.

4 Biogas flow rate

We recall that the biogas flow rate is proportional to the microbial activity, as defined for instance in [3, 27]. We consider here the biogas flow rate as a function of the input substrate concentration S^{in}, the dilution rate D and the parameter r.

For $r(f(S^{in}) - a) \le D < (1-r)(f(S^{in}) - a)$, the biogas flow rate corresponding to the steady state E_1 is given by the expression

$$G_1(S^{in}, D, r) = V_2\overline{x}_2 f(\overline{S}_2), \tag{36}$$

with $V_2 = (1-r)V$, $\overline{x}_2$ and $\overline{S}_2$ defined in (64).

For $D < r(f(S^{in}) - a)$, the biogas flow rate corresponding to the positive steady state E_2 is given by the expression

$$G_2(S^{in}, D, r) = V_1 x_1^* f(S_1^*) + V_2 x_2^* f(S_2^*), \tag{37}$$

with $V_1 = rV$, $V_2 = (1-r)V$, x_1^* and S_1^* defined in (66), x_2^* defined by (67) and S_2^* the unique solution of $h(S_2) = f(S_2)$.

Proposition 4. *1. When $r(f(S^{in}) - a) \le D$ and $D < (1-r)(f(S^{in}) - a)$ then*

$$G_1(S^{in}, D, r) = VD(S^{in} - \overline{S}_2). \tag{38}$$

2. When $D < r(f(S^{in}) - a)$ then

$$G_2(S^{in}, D, r) = VD(S^{in} - S_2^*). \tag{39}$$

Proof. From system (59), considering equation $\dot{S}_2 = 0$, one obtains $\overline{x}_2 f(\overline{S}_2) = D(S^{in} - \overline{S}_2)/(1-r)$. Thus,

$$G_1(S^{in}, D, r) = V_1 \frac{D}{r}(S^{in} - \overline{S}_2) = VD(S^{in} - \overline{S}_2).$$

From system (59), considering $\dot{S}_1 = 0$ and $\dot{S}_2 = 0$ gives respectively $x_1^* f(S_1^*) = D(S^{in} - S_1^*)/r$ and $x_2^* f(S_2^*) = D(S_1^* - S_2^*)/(1-r)$. Thus, one has

$$\begin{aligned} G_2(S^{in}, D, r) = \ & V_1 \frac{D}{r}(S^{in} - S_1^*) + V_2 \frac{D}{1-r}(S_1^* - S_2^*) \\ = \ & VD(S^{in} - S_2^*). \end{aligned}$$

This ends the proof of the proposition. $\qquad\square$

Although $G_1(S^{in}, D, r)$ and $G_2(S^{in}, D, r)$, given by (36) and (37), respectively, are not defined for $r = 0$ or $r = 1$, the formulas (38) and (39) allow them to be extended to $r = 0$ and $r = 1$, as was done for S_r^{out} in (6). We can write

$$G_1(S^{in}, D, 0) = G_2(S^{in}, D, 1) = G_{chem}(S^{in}, D),$$

where

$$G_{chem}(S^{in}, D) = VD(S^{in} - \lambda(D + a)), \tag{40}$$

represents the biogas flow rate of the single chemostat when $0 < D < f(S^{in}) - a$. For more information on $G_{chem}(S^{in}, D)$, see (56) in Appendix A.
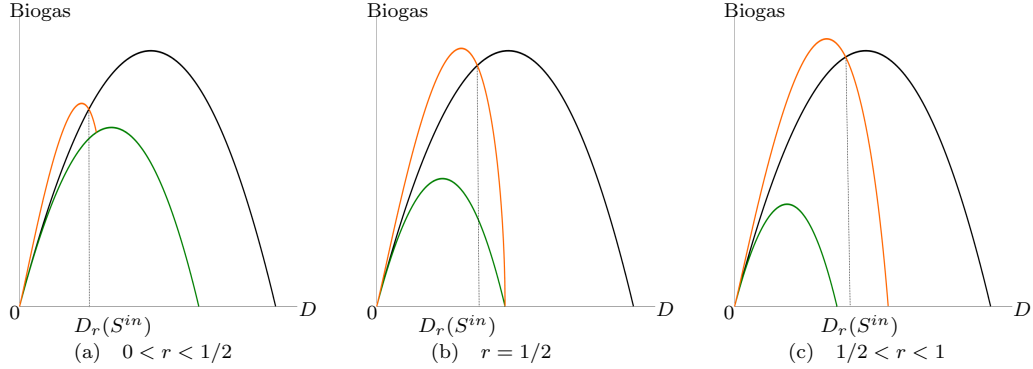
Figure 5: For r and S^{in} fixed, the curves of the maps $D \mapsto G_1(S^{in}, D, r)$, in green, $D \mapsto G_2(S^{in}, D, r)$, in orange, and $D \mapsto G_{chem}(S^{in}, D)$, in black, where G_1, G_2 and G_{chem} are given by (38), (39) and (40) respectively.
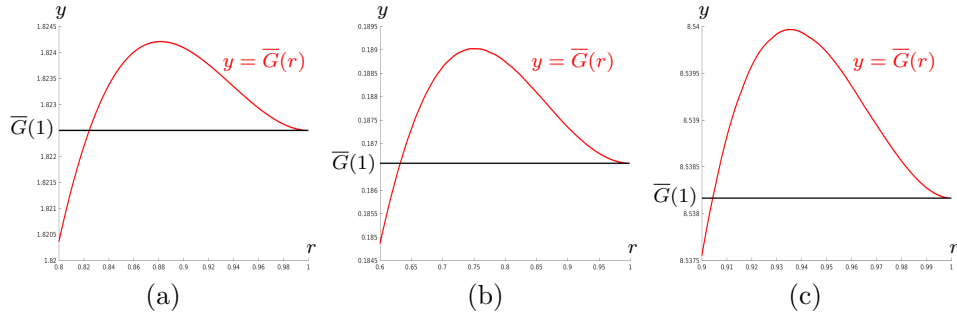
Figure 6: The map $r \mapsto \overline{G}(r)$ with $\overline{G}$ defined by (42). (a) $f(S) = 4S$, $a = 0.6$ and $S^{in} = 1.5$. (b) $f(S) = 4S/(5 + S)$, $a = 0.3$ and $S^{in} = 1.5$. (c) $f(S) = 4S^2/(25 + S^2)$, $a = 0.3$ and $S^{in} = 10$.

4.1 The serial configuration can be more efficient than the single chemostat

In this section, we prove that the biogas flow rate G_1 corresponding to the steady state E_1 is always smaller than the biogas flow rate of the single chemostat. However, the biogas flow rate G_2 corresponding to the steady state E_2 can be larger than the biogas flow rate of the single chemostat. More precisely, we have the following result.

Proposition 5. *Assume that Assumption 1 is satisfied. Let $r \in (0, 1)$, $0 \le D < f(S^{in}) - a$ and G_{chem} defined by (40).*

1. *If $r(f(S^{in}) - a) \le D$ and $D < (1 - r)(f(S^{in}) - a)$, then $G_1(S^{in}, D, r) < G_{chem}(S^{in}, D)$, where G_1 is given by (38).*

15

2. If $D < r(f(S^{in}) - a)$, then

$$G_2(S^{in}, D, r) > G_{chem}(S^{in}, D) \Longleftrightarrow S^{in} > g_r(D),$$

where G_2 is given by (39) and g_r is defined by (9).

- *If, in addition, Assumption 2 is satisfied, and $S^{in} > g(D)$, then $G_2(S^{in}, D, r) > G_{chem}(S^{in}, D)$, if and only if $r > r_1(S^{in}, D)$, where $r_1(S^{in}, D)$ is defined by (20).*
- *If, in addition, Assumption 3 is satisfied, then $G_2(S^{in}, D, r) > G_{chem}(S^{in}, D)$, if and only if $D < D_r(S^{in})$, where $D_r(S^{in})$ is defined by (25).*

Proof. 1. Since $D/(1-r) > D$ and λ is increasing, we have $\lambda(D/(1-r)+a) > \lambda(D+a)$. Then, using the formula for G_1 given in Proposition 4, this induces the inequality $G_1(S^{in}, D, r) < G_{chem}(S^{in}, D)$.

2. According to Theorem 1, for any $r \in (0, 1)$ and $D < r(f(S^{in}) - a)$ one has $S_2^*(S^{in}, D, r) < \lambda(D + a)$ if and only if $S^{in} > g_r(D)$. Consequently, using the formula for G_2 given in Proposition 4, one has $G_2(S^{in}, D, r) > G_{chem}(S^{in}, D)$ if and only if $S^{in} > g_r(D)$. If Assumption 2 is satisfied, then, using (21), we see that $G_2(S^{in}, D, r) > G_{chem}(S^{in}, D)$ if and only if $r > r_1(S^{in}, D)$. If Assumption 3 is satisfied, then, using (26), we see that $G_2(S^{in}, D, r) > G_{chem}(S^{in}, D)$ if and only if $D < D_r(S^{in})$.
This ends the proof of the proposition. $\qquad\square$

Let S^{in} and D be fixed. The graphs of the biogas flow rates functions

$$r \mapsto G_1(S^{in}, D, r), \text{ and } r \mapsto G_2(S^{in}, D, r),$$

are easily obtained from the graph of the output substrate concentration, $r \mapsto S_r^{out}(S^{in}, D)$, see Fig. 4. Indeed, the formulas given in Proposition 4 show that, whenever these functions are defined, we have

$$
\begin{aligned}
G_1(S^{in}, D, r) &= VD\left(S^{in} - S_r^{out}(S^{in}, D)\right), \\
G_2(S^{in}, D, r) &= VD\left(S^{in} - S_r^{out}(S^{in}, D)\right).
\end{aligned}
$$

We will see in Section 5, some illustrative plots of the biogas flow rates G_1 and G_2 as functions of the parameter $r \in [0, 1]$, for linear growth, see Fig. 7, Monod growth, see Fig. 8 and Hill growth, see Fig. 9.

Let us illustrate the result of Proposition 5 by plotting the graphs of the biogas flow rates

$$D \mapsto G_1(S^{in}, D, r) \text{ and } D \mapsto G_2(S^{in}, D, r),$$

when r and S^{in} are fixed, see Fig. 5. This figure is made without graduations on the axes because its represents a general situation where the growth function is only assumed to verify our hypotheses. Indeed the behaviors of the functions, depicted in this figure, follow from our results and are not simply numerical illustrations.

Notice that for any $r \in (0, 1)$, the graph of G_1 (plotted in green in the figure) is always below the graph G_{chem} (plotted in black). This illustrates item 1 of Proposition 5. Assuming that Assumption 3 is satisfied, then for all $0 < D < D_r(S^{in})$, the graph of G_2 (plotted in orange) is above the graph of G_{chem} (plotted in black). This illustrates item 2 of Proposition 5.

4.2 The maximal biogas of the serial configuration can exceed that of the single chemostat

In Figure 5(c) the plot shows that the maximum of G_2 (the red curve) is larger than the maximum of G_{chem}, as we want to emphasize that the following inequality is possible

$$\max_D G_2(S^{in}, D, r) > \max_D G_{chem}(S^{in}, D). \tag{41}$$

Indeed we will show that there is a value $r^* \in (0,1)$ such that this inequality is true for all $r \in (r^*, 1)$. The treshold r^* obviously depends on S^{in} and the the rate of mortality a. It will be noted $r^*(S^{in}, a)$ when we want to highlight this dependence. This phenomenon never never occurs in the case of no mortality, since we have $r^*(S^{in}, 0) = 1$. Indeed, in the case without mortality, we proved, see Proposition 6 of [7], that for all $S^{in} > 0$, and all $r \in (0, 1)$ we have

$$\max_D G_2(S^{in}, D, r) < \max_D G_{chem}(S^{in}, D),$$

that is to say, the maximal biogas flow rate of the serial configuration never exceed the maximal biogas flow rate of the single chemostat.

Let us we prove that, when $a > 0$, the inequality (41) is always true for r sufficiently close to 1. Observe that for any fixed $S^{in} > \lambda(a)$ and $r \in (0, 1]$, the continuous function $D \mapsto G_2(S^{in}, D, r)$ is defined on the closed interval $\left[0, r\left(f(S^{in}) - a\right)\right]$. It is null at the extremities of this interval and positive on the open interval $\left(0, r\left(f(S^{in}) - a\right)\right)$. Therefore, it reaches it maximum. For a given $S^{in} > \lambda(a)$, we then consider the function

$$\overline{G}(r) := \max_{D \in [0, r(f(S^{in}) - a)]} G_2(S^{in}, D, r). \tag{42}$$

We want to ensure that this maximum is reached at a single value, denoted $\overline{D}(r)$. Note that $\overline{D}(1)$ represents the value, which we will assume to be unique, at which the function $D \mapsto G_{chem}(S^{in}, D)$ reaches its maximum. We need the following assumption.

Assumption 4. *The function f is C^2 and increasing and, for $S^{in} > \lambda(a)$, there exists $\overline{D}(1) \in (0, f(S^{in}) - a)$ such that $D \mapsto G_{chem}(S^{in}, D)$ is*

- *strictly concave at $\overline{D}(1)$,*

- *increasing on $(0, \overline{D}(1))$,*

- *decreasing on $(\overline{D}(1), f(S^{in}) - a)$,*

These conditions are related to the single chemostat model. They are verified for linear, Monod, or Hill growth functions, see Remark 3 in Appendix A.

If Assumption 4 is satisfied, then the maximum of the function $D \mapsto G_{chem}(S^{in}, D)$ is unique. The following lemma shows that the function $D \mapsto G_2(S^{in}, D, r)$ satisfies the same property for r sufficiently close to 1.

Lemma 4. *Assume that Assumption 4 is satisfied, then for any $S^{in} > \lambda(a)$, there exists a neighborhood $\mathcal{V}_1$ of 1, such that for any $r \in \mathcal{V}_1 \cap \{r \le 1\}$, the maximum of the function $D \mapsto G_2(S^{in}, D, r)$ is unique. We denote it by $\overline{D}(r)$. Moreover, $\overline{D}$ is differentiable on $\mathcal{V}_1 \cap \{r < 1\}$ with bounded derivative.*

Proof. The proof is given in in Appendix D.2. □

Proposition 6. *Under Assumption 4, the function $\overline{G}$ admits left limits of its first and second derivatives at $r = 1$, which are*

$$\begin{aligned} &\overline{G}'(1^-) = 0, \\ &\overline{G}''(1^-) = \tfrac{2a\overline{D}(1)}{\overline{D}(1) + a}\left(S^{in} - \lambda(\overline{D}(1) + a)\right). \end{aligned} \tag{43}$$

Proof. The proof is given in Appendix D.3. □

Proposition 7. *Under Assumption 4, there exists r^* in $(0, 1)$ such that (41) is true for any $r \in (r^*, 1)$ and*
$$\max_D G_2(S^{in}, D, r^*) = \max_D G_{chem}(S^{in}, D).$$

Proof. From Proposition 6, there exist $\varepsilon > 0$ such that for all $r \in (1-\varepsilon, 1)$, we have $\overline{G}(r) > \overline{G}(1)$. Therefore, the subset I of $(0,1)$ defined by

$$I = \{\rho \in (0,1) : \forall r \in (\rho, 1), \overline{G}(r) > \overline{G}(1)\},$$

is non empty. Let r^* be the lower bound of I. We have $\overline{G}(r^*) = \overline{G}(1)$ and $\overline{G}(r) > \overline{G}(1)$ for $r \in (r^*, 1)$. Using (42), we deduce that the equality in the proposition is true and (41) is true for any $r \in (r^*, 1)$. $\qquad\square$

The function $r \mapsto \overline{G}(r)$ reaches its maximum at some $r^{max} \in (r^*, 1)$. Let $D^{max} = \overline{D}(r^{max})$ be the maximum of the function $D \mapsto G_2(S^{in}, D, r^{max})$. Therefore the maximal biogas flow rate of the serial chemostat is given by $G_2(S^{in}, D^{max}, r^{max})$. It satisfies

$$G_2(S^{in}, D^{max}, r^{max}) > G_{chem}\left(S^{in}, \overline{D}(1)\right).$$

We have plotted the function $r \mapsto \overline{G}(r)$ for the linear, Monod, and Hill growth functions considered in Fig. 6. It is seen in this figure that the tangent at $r = 1$ is horizontal which corresponds to $\overline{G}'(1) = 0$. In addition, one remarks that $\overline{G}(r) > \overline{G}(1)$ for r in some interval $(r^*, 1)$ and $\overline{G}(r^*) = \overline{G}(1)$. Thus, with presence of mortality rate, if practitioners are able to choose the dilution rate D, the good strategy consists in working with a serial configuration and choose r in the interval $(r^*, 1)$. The serial configuration should be operated at $D = \overline{D}(r)$, where $\overline{D}(r)$ is defined in Lemma 4.

Remark 2.
- *If one is interested in increasing the flow of biogas, the best choice is $r = r^{max}$, $D = D^{max}$.*

- *If one is interested in reducing the dilution rate, the best choice is $r = r^*$ and $D = D^*$, where $D^* = \overline{D}(r^*)$.*

Indeed, for the choice $r = r^*$ and $D = D^*$, we have

$$G_2(S^{in}, D^*, r^*) = G_{chem}\left(S^{in}, \overline{D}(1)\right),$$

but D^* is expected to be significantly smaller than $\overline{D}(1)$, the dilution rate that maximises biogas for the simple chemostat. In fact, reducing D means that the flow rate Q has been reduced, and therefore energy has been saved to obtain the same result as with a simple chemostat

This result has an important message for practitioners: the serial configuration is worth considering when mortality is not negligible. To the best of our knowledge, this result is new in the literature. On the other hand, it is not intuitive. For more information on this issue, see Section 5.4. For biolobical comments on the heuristic underlying this non-intuitive behaviour, the reader is refered to [6].

5 Illustrations and numerical simulations

This section illustrates of results using three different growth functions. As concave functions, we choose the linear growth function and the Monod function. As a non concave function, we choose the Hill function.

5.1 Linear growth function

Let consider a linear function $f(S) = \alpha S$, $\alpha > 0$. As it is concave, according to item ii in Remark 1, the linear function verifies Assumptions 2 and 3. Therefore, our results apply for a linear function.

One has $\lambda(2D+a) = g(D) = (2D+a)/\alpha$ then, the curves $\Phi_{1/2}$, defined by (13), and Γ, defined by (22), are identical. Consequently, the operating plane (S^{in}, D) is divided in three regions J_i, $i = 0, 1, 3$ defined in (23) that describe the behavior of the output substrate concentration and the biogas flow rate, see Figure 7(a).
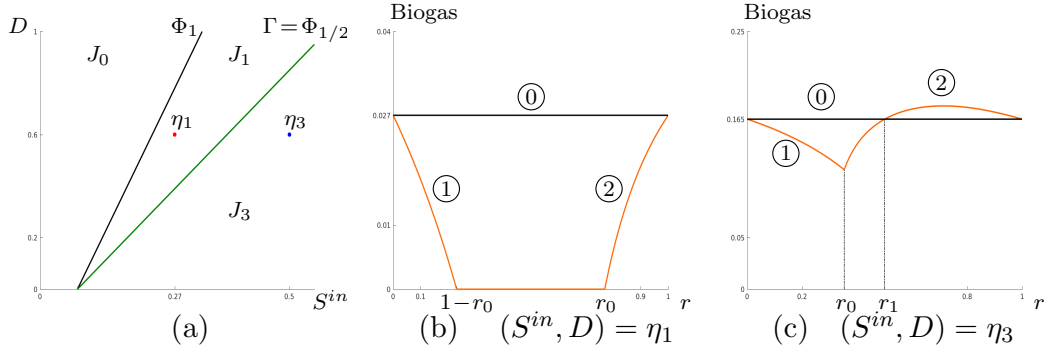
Figure 7: (a) The regions J_0, J_1 and J_3 of the operating plane with $f(S) = 4S$ and $a = 0.3$. The biogas flow rates corresponding to points $\eta_1 = (0.27, 0.6) \in J_1$ and $\eta_3 = (0.5, 0.6) \in J_3$ are depicted in panels (b) and (c) respectively. In these panels, the numbered curves ⓪ (in black), and ①, ② (in orange) are respectively defined by $y = G_{chem}(S^{in}, D)$, $y = G_1(S^{in}, D, r)$ and $y = G_2(S^{in}, D, r)$; $r_0(S^{in}, D) = D/(f(S^{in}) - a)$ and $r_1(S^{in}, D)$ is defined by (20). (b) $r_0 \approx 0.77$. (c) $r_0 \approx 0.35$ and $r_1 = 0.5$.
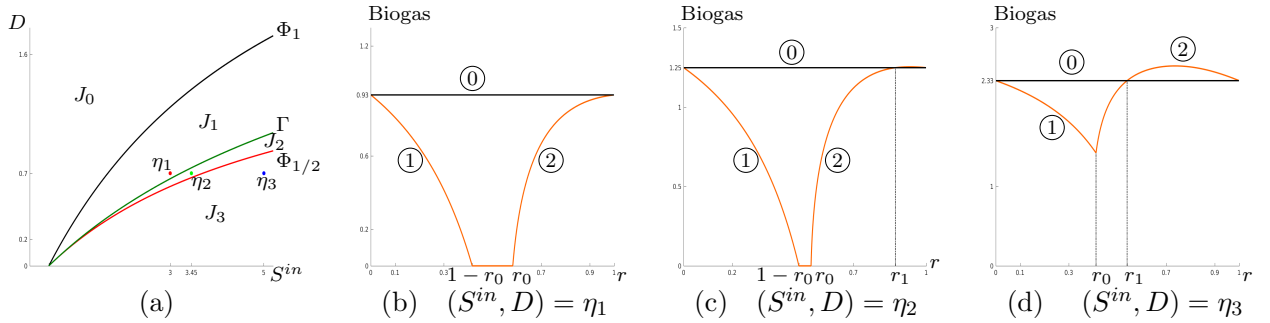

Figure 8: (a) The regions J_0, J_1 J_2 and J_3 in the operating plane with $f(S) = 4S/(5 + S)$ and $a = 0.3$. The biogas flow rates corresponding to points $\eta_1 = (3, 0.7) \in J_1$, $\eta_2 = (3.45, 0.7) \in J_2$ and $\eta_3 = (5, 0.7) \in J_3$ are depicted in panels (b), (c) and (d) respectively. In these panels the curves are coloured and numbered as in Fig. 7, $r_0(S^{in}, D) = D/(f(S^{in}) - a)$, and $r_1(S^{in}, D)$ is defined by (20) (b) $r_0 \approx 0.58$. (c) $r_0 \approx 0.53$ and $r_1 \approx 0.87$. (d) $r_0 \approx 0.41$ and $r_1 \approx 0.54$.

Consider the operating points η_1 and η_3, fixed respectively in regions J_1 and J_3, as shown in Figure 7(a). The behavior of the biogas flow rate for these operating points is depicted in Figure 7(b,c). It should be noticed that for any other point $(S^{in}, D) \in J_1$, the curve representing the biogas flow rate with respect to r should be similar to the curve shown in Figure 7(a), and corresponding to $(S^{in}, D) = \eta_1$. Similarly, for any other point $(S^{in}, D) \in J_3$, it should be similar to the curve shown in Figure 7(b), and corresponding to $(S^{in}, D) = \eta_3$.

In the linear case, the equation $S^{in} = g_r(D)$ is a second degree algebraic equation in r that gives two solutions, one corresponds to $r_1(S^{in}, D)$ defined by (20) and the other one is not considered as it does not belong to $(0, 1)$.

Since the point $\eta_3 = (0.5, 0.6)$ satisfies the condition $S^{in} > g(D)$, as stated in item 2 of Proposition 5, the serial configuration has a higher biogas flow rate production than a single chemostat if and only if $r \in (r_1, 1)$, where $r_1(0.5, 0.6) \approx 0.5$, see Figure 7 (b).

5.2 Monod function

The Monod function is $f(S) = mS/(K + S)$. As it is concave, according to item ii in Remark 1, the Monod function verifies Assumptions 2 and 3. Therefore, our results apply for Monod function.

19

Lemma 5. *For any $D > 0$, the curve Γ, defined by (22), is at left of the curve $\Phi_{1/2}$, defined by (13).*

Proof. The curves $\Phi_{1/2}$ and Γ are respectively defined by equations $S^{in} = \lambda(2D + a)$ and $S^{in} = g(D)$. Let the function $H : [0, (m-a)/2] \mapsto \mathbb{R}$ be defined by

$$H(D) = \lambda(2D + a) - g(D) = \frac{KmD^2}{(m-D-a)^2(m-a-2D)}.$$

Note that $H(0) = 0$ and, for any $D \in (0, (m-a)/2)$, one has $H(D) > 0$ i.e. $\lambda(2D + a) > g(D)$.

Hence, the curve Γ is at left of the curve $\Phi_{1/2}$. $\qquad\square$

As a consequence of Lemma 5, the operating plane (S^{in}, D) is divided in four regions J_i, $i = 0, 1, 2, 3$ defined in (23) that describe the behavior of the output substrate concentration and the biogas flow rate, see Fig. 8(a).

Consider the operating points η_1, η_2 and η_3, fixed respectively in regions J_1, J_2 and J_3, as shown in Fig. 8(a). The behavior of the biogas flow rate for these points is depicted in Fig. 8(b,c,d). It should be noticed that for any other point $(S^{in}, D) \in J_1$ (resp. $(S^{in}, D) \in J_2$ and $(S^{in}, D) \in J_3$), the curve representing the biogas flow rate with respect to r should be similar to the curve shown in Fig. 8(b) (resp. 8(c) and 8(d)), and corresponding to $(S^{in}, D) = \eta_1$ (resp. $(S^{in}, D) = \eta_2$ and $(S^{in}, D) = \eta_3$).

In the Monod case, the equation $S^{in} = g_r(D)$ is a second degree algebraic equation in r that gives two solutions, one corresponds to $r_1(S^{in}, D)$ defined by (20) and the other one is not considered as it does not belong to $(0, 1)$.

Since the point η_2 (resp. η_3) satisfies the condition $S^{in} > g(D)$, as stated in item 2 of Proposition 5, the serial configuration has a higher biogas flow rate production than a single chemostat if and only if $r \in (r_1, 1)$, with $r_1(3.45, 0.7) \approx 0.87$ in Fig.8(c) and $r_1(5, 0.7) \approx 0.54$ in Fig. 8(c).

5.3 Hill function

The Hill function is $f(S) = mS^p/(K^p + S^p)$. Note that if $p = 1$ this function reduces to the Monod function. For $p > 1$ it is non-concave. We have

$$\lambda(a) = \left(\frac{a}{m-a}\right)^{1/p} K.$$

Proposition 8. *The Hill function satisfies the conditions (34) and (35). Therefore, according to item iii in Remark 1, it verifies Assumption 2 and according to Lemma 3, it satisfies Assumption 3.*

Proof. Let us first prove that the Hill function satisfies the condition (35). Straightforward computation give

$$\frac{d^2}{dS^2}\left(\frac{1}{f(S)-a}\right) = mpK^p \frac{(p+1)(m-a)S^{2p-2}+(p-1)aK^pS^{p-2}}{((m-a)S^p-aK^p)^3}.$$

Therefore, $\frac{d^2}{dS^2}\left(\frac{1}{f(S)-a}\right) > 0$ for all $S > \lambda(a)$, that is to say, (35) is satisfied. This result can also be obtained without laborious calculations by using item *iii* of Remark 1. Let $\hat{S} \in (0, +\infty)$ be the inflexion point of the Hill function f. It is sufficient to show that $(1/f)'' > 0$ for all $S \in (0, \hat{S})$. One easily see that

$$\left(\frac{1}{f}\right)''(S) = \frac{p(p+1)K^p}{mS^{p+2}} > 0,$$

for any $S > 0$. Consequently, for all $p > 1$, the Hill function verifies Assumption 2.

Let us now prove that the Hill function verifies the condition (34). Straightforward computations give

$$f'(\lambda(D+a)) = \frac{p}{Km}(D+a)^{\frac{p-1}{p}}(m-a-D)^{\frac{p+1}{p}}. \tag{44}$$
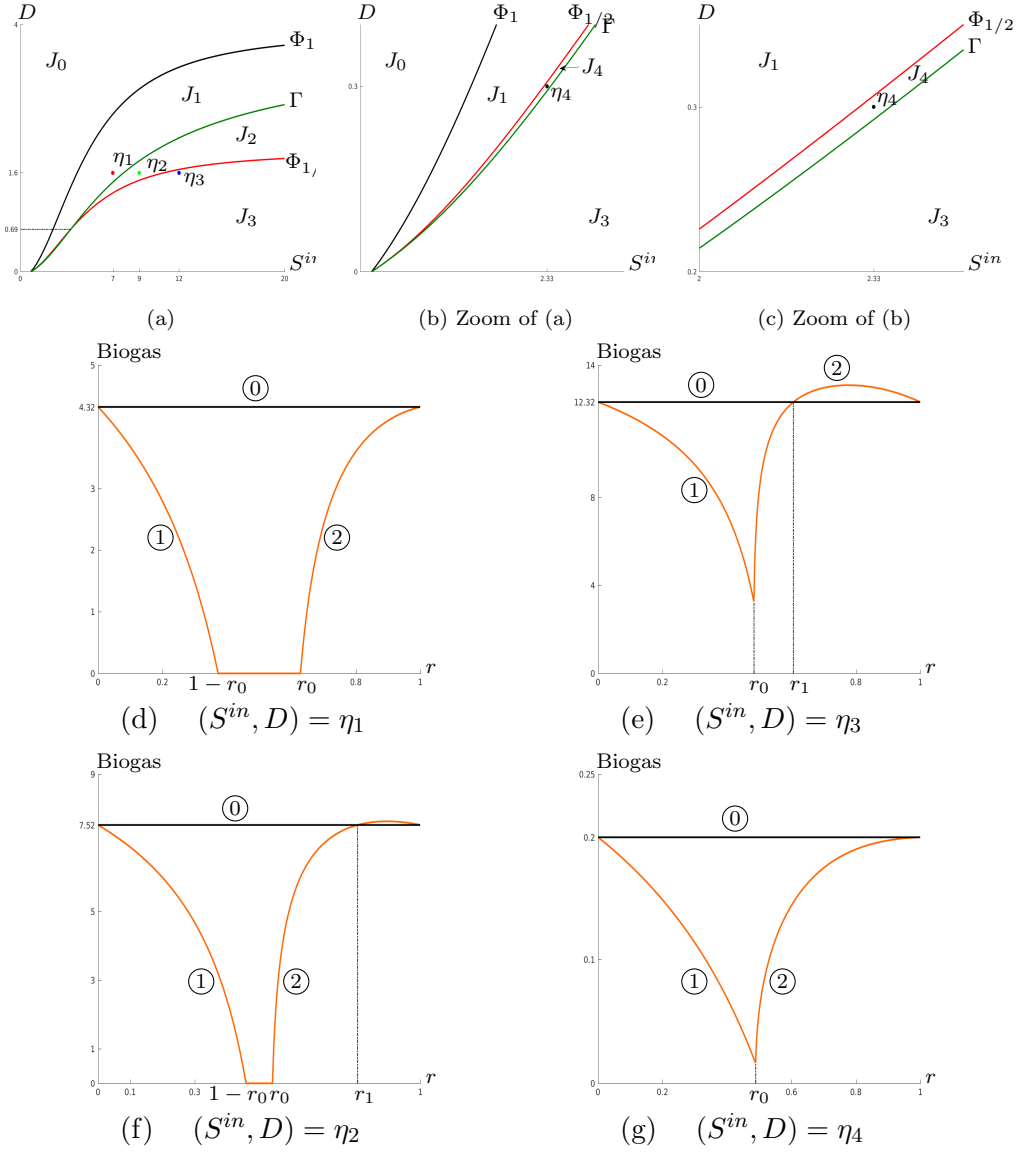
Figure 9: (a) The regions J_0, J_1 J_2, J_3 and J_4 in the operating plane with $f(S) = 4S^2/(25 + S^2)$ and $a = 0.1$. The curves Γ and $\Phi_{1/2}$ intersects for $D_1 = 0.69$ (see Lemma 6). (b,c) Zooms of (a) showing the region J_4. The biogas flow rates corresponding to points $\eta_1 = (7, 1.6) \in J_1$, $\eta_2 = (9, 1.6) \in J_2$, $\eta_3 = (12, 1.6) \in J_3$ and $\eta_4 = (2.33, 0.3) \in J_4$ are depicted in panels (d) to (g), respectively. In these panels curves are coloured and numbered as in Fig. 7, $r_0(S^{in}, D) = D/(f(S^{in}) - a)$, and $r_1(S^{in}, D)$ is defined by (20). (d) $r_0 \approx 0.63$. (e) $r_0 \approx 0.54$ and $r_1 \approx 0.81$. (f) $r_0 \approx 0.48$ and $r_1 \approx 0.61$. (g) $r_0 \approx 0.49$.

Therefore,

$$f'\left(\lambda\left(\tfrac{D}{r} + a\right)\right) = \tfrac{p}{Km}\left(\tfrac{D}{r} + a\right)^{\frac{p-1}{p}}\left(m - a - \tfrac{D}{r}\right)^{\frac{p+1}{p}}.$$

Since $p > 1$, $D + ra < D + a$ and

$$0 < rm - ra - D < m - a - D,$$

one has

$$(D + ra)^{\frac{p-1}{p}} < (D + a)^{\frac{p-1}{p}} \tag{45}$$

$$(rm - ra - D)^{\frac{1}{p}} < (m - a - D)^{\frac{1}{p}}. \tag{46}$$

From (45) one has

21

$$\left(\frac{D}{r} + a\right)^{\frac{p-1}{p}} = \left(\frac{1}{r}\right)^{\frac{p-1}{p}} (D + ra)^{\frac{p-1}{p}} < \left(\frac{1}{r}\right)^{\frac{p-1}{p}} (D + a)^{\frac{p-1}{p}}. \tag{47}$$

On the other hand, we have

$$\left(m - a - \frac{D}{r}\right)^{\frac{p+1}{p}} = \left(\frac{1}{r}\right)^{\frac{1}{p}} \left(m - a - \frac{D}{r}\right) A,$$

where $A = (rm - ra - D)^{\frac{1}{p}}$. From (46), and using

$$0 < m - a - D/r < m - a - D,$$

we then deduce

$$\left(m - a - \frac{D}{r}\right)^{\frac{p+1}{p}} < \left(\frac{1}{r}\right)^{\frac{1}{p}} (m - a - D)^{\frac{p+1}{p}}. \tag{48}$$

Therefore, using (44), (47) and (48) one obtains

$$\begin{aligned} f'\left(\lambda\left(\frac{D}{r} + a\right)\right) &= \frac{p}{Km}\left(\frac{D}{r} + a\right)^{\frac{p-1}{p}}\left(m - a - \frac{D}{r}\right)^{\frac{p+1}{p}} \\ &< \frac{p}{Km}\frac{1}{r}(D + a)^{\frac{p-1}{p}}(m - a - D)^{\frac{p+1}{p}} = \frac{1}{r}f'(\lambda(D + a)). \end{aligned}$$

This ends the proof of (34). Consequently, according to Lemma 3, any Hill function satisfies Assumption 3. $\qquad\square$
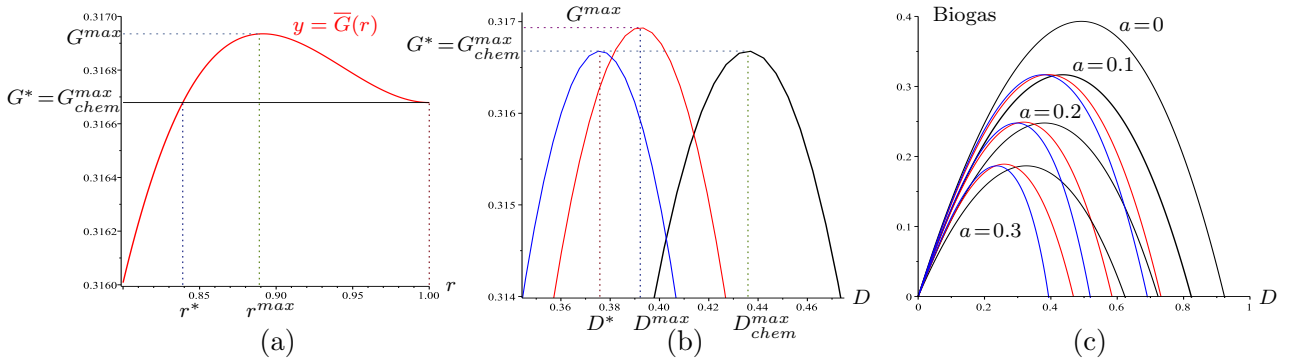
Figure 10: (a) The map $r \mapsto \overline{G}(r)$ defined by (42), with $f(S) = 4S/(5 + S)$, $a = 0.1$ and $S^{in} = 1.5$, showing the values r^* and r^{max}. (b) The corresponding maps $D \mapsto G_{chem}(S^{in}, D)$, in black, $D \mapsto G_2(S^{in}, D, r^*)$, in blue and $D \mapsto G_2(S^{in}, D, r^{max})$, in red, show the values $D* < D^{max} < D^{max}_{chem}$. (c) The biogas flow rates for $a = 0, 0.1, 0.2, 0.3$ showing the effects of mortality.

Let now consider the case $p = 2$ of the Hill function: $f(S) = mS^2/(K^2 + S^2)$.

Lemma 6. *Let* $D_1 = (3m - 4a - \sqrt{m(5m - 4a)})/4$. *If* $0 < D < D_1$ *then the curve* $\Phi_{1/2}$, *defined by (13), at left of the curve* Γ, *defined by (22). In contrast, if* $D_1 < D < (m - a)/2$ *then the curve* $\Phi_{1/2}$ *is at right of the curve* Γ.

Proof. Let the function $H : [0, (m - a)/2] \mapsto \mathbb{R}$ be defined by $H(D) := \lambda(2D + a) - g(D)$. We have

$$H(D) = K\left(\sqrt{\frac{2D+a}{m-a-D}} - \frac{(2D+a)(m-a-D)+(D+a)(m-a)}{2(m-a-D)^{3/2}\sqrt{D+a}}\right).$$

Straightforward computation shows that this function is positive if and only if the polynomial

$$Q(D) := 4D^2 - 2(3m - 4a)D + 4a^2 - 5am + m^2$$

is negative. The solution of equation $Q(D) = 0$ are

$$D_1 = \frac{3m - 4a - \sqrt{\Delta}}{4} \text{ and } D_2 = \frac{3m - 4a + \sqrt{\Delta}}{4},$$

where $\Delta = 4m(5m - 4a) > 0$, as $a < m$. Notice that we have $0 < D_1 < (m - a)/2$ and $(m - a)/2 < D_2$. Thus, for any $D \in (D_1, (m - a)/2)$, we have $H(D) > 0$ and then the curve $\Phi_{1/2}$ at right of the curve Γ. $\square$

As a consequence of Lemma 6, the operating plane is divided in five regions J_i $i = 0, 1, 2, 3, 4$ defined in (23), see Figure 9(a,b,c).

Consider the operating points η_1, η_2, η_3 and η_4 fixed respectively in regions J_1, J_2, J_3 and J_4, as shown in Figure 9(a,b,c). It should be noticed that for any other point $(S^{in}, D) \in J_1$ (resp. $(S^{in}, D) \in J_2$, $(S^{in}, D) \in J_3$ and $(S^{in}, D) \in J_4$), the curve representing the biogas flow rate with respect to r should be similar to the curve shown in Fig. 9(a) (resp. (b), (c) and (d)), and corresponding to $(S^{in}, D) = \eta_1$ (resp. $(S^{in}, D) = \eta_2$, $(S^{in}, D) = \eta_3$ and $(S^{in}, D) = \eta_4$).

Recall that $r_1(S^{in}, D)$ is defined by (20). It is obtained by solving numerically the equation $S^{in} = g_r(D)$. Since the point η_2 (resp. η_3) satisfies the condition $S^{in} > g(D)$, as stated in item 2 of Proposition 5, the serial configuration has a higher biogas flow rate production than a single chemostat if and only if $r \in (r_1, 1)$, with $r_1(9, 1.6) \approx 0.81$ in Fig. 9(e) and $r_1(12, 1.6) \approx 0.61$, in Fig. 9(f).

5.4 The serial configuration is worth considering when mortality is not negligible

In this section we numerically illustrate Remark 2. We fix S^{in} and we adopt the following notations.

$$D_{chem}^{max} = \overline{D}(1), \quad G_{chem}^{max} = \overline{G}(1) = G_{chem}\left(S^{in}, D_{chem}^{max}\right)$$

where $\overline{G}(r)$ is defined by (42) and $\overline{D}(r)$ is as in Lemma 4. Recall that $r^* \in (0, 1)$ satisfies

$$\overline{G}(r^*) = \overline{G}(1) = G_{chem}^{max}, \tag{49}$$

and $\overline{G}(r) > \overline{G}(1)$ for $r \in (r^*, 1)$, so that $\overline{G}(r)$ attains its maximum for $r = r^{max} \in (r^*, 1)$, see Fig. 10(a), obtained with a Monod function and $S^{in} = 1.5$. We adopt the following notations.

$$D^{max} = \overline{D}(r^{max}), \quad G^{max} = G_2\left(S^{in}, D^{max}, r^{max}\right)$$
$$D^* = \overline{D}(r^*), \quad G^* = G_2\left(S^{in}, D^*, r^*\right) = G_{chem}^{max}$$

Table 1: Numerical values

	$a = 0$	$a = 0.1$	$a = 0.2$	$a = 0.3$
D_{chem}^{max}	0.4918	0.4359	0.3806	0.3259
$G^* = G_{chem}^{max}$	0.3930	0.3167	0.2478	0.1866
r^*	1	0.839	0.717	0.631
D^*	0.4918	0.3758	0.2969	0.2369
r^{max}	1	0.889	0.808	0.751
D^{max}	0.4918	0.3925	0.3190	0.2591
G^{max}	0.3930	0.3169	0.2490	0.1890
$\frac{G^{max} - G_{chem}^{max}}{G_{chem}^{max}}$	0	0.06%	0.5%	1.3%
$\frac{D_{chem}^{max} - D^{max}}{D_{chem}^{max}}$	0	10%	16.2%	20.5%
$\frac{D_{chem}^{max} - D^*}{D_{chem}^{max}}$	0	13.6%	22%	27.3%

These notations are illustrated in Figs. 10(a,b). The zoom in Fig. 10(b) shows that G^{max} exceeds $G^* = G^{max}_{chem}$ only slightly, but D^* is significantly smaller than D^{max}, which is itself smaller than D^{max}_{chem}. We give in Table 1 the numerical values of r^*, r^{max}, D^*, D^{max}, G^{max} and $G^* = G^{max}_{chem}$, for various values of the mortality rate a. The table also gives the relative gains

$$\frac{G^{max}-G^{max}_{chem}}{G^{max}_{chem}}, \qquad \frac{D^{max}_{chem}-D^{max}}{D^{max}_{chem}}, \qquad \frac{D^{max}_{chem}-D^*}{D^{max}_{chem}},$$

when replacing the single chemostat with the serial device using the ratios r^* and r^{max}. The gain in biogas production is almost negligible, but the gain in bioreactor flow rate is significant.

The biogas flow rates $G_{chem}(S^{in}, D)$, $G_2(S^{in}, D, r^*)$ and $G_2(S^{in}, D, r^{max})$, for the various considered values of the mortality rate a, are depicted in Fig. 10(c), in black, blue and red, respectively. This figure shows that mortality is a real problem as it considerably reduces biogas production. Where mortality cannot be avoided or reduced, instead of using the single chemostat, by using a serial device, biogas production can be slightly improved while significantly reducing the bioreactor flow rate.

6   Conclusion

In this work, an in-depth study is carried out on the mathematical model of two interconnected chemostats in serial with mortality. Equations contain a term representing the mortality rate of the species. Due to this added term characterizing the mathematical model, this paper is considered as an extension of the work done in [7], where the model does not consider the mortality rate. However, the mathematical analysis revealed that the proofs have had to be significantly revisited and reveal several new non intuitive differences compared to the case without mortality. Let us recall that without mortality, the dynamics admits a forward attractive invariant hyperplane related to the total mass conservation, which is no longer verified under mortality consideration. This at the core of the differences in the mathematical analysis. The study of the model is based on the analysis of the asymptotic behavior of its solutions, and is supported by an operating diagram which describes the number and stability of steady states. In a first step, we considered different mortality rates a_1, a_2 in each tank. Then, in view of comparing with the single configuration, we considered identical mortality rate $a = a_1 = a_2$. We analyzed the performances of the model at steady state for two different criteria: the output substrate concentration and the biogas flow rate (and compared them for the single chemostat with the same mortality rate a). Explicit expressions of criteria, depending on the dilution rate D and the input substrate concentration S^{in}, are provided. These new results provide conditions that insure the existence of a serial configuration more efficient than a single chemostat, in the sense of minimizing the output substrate concentration or maximizing the biogas flow rate.

Along the paper, the similarities, specificities and differences of our model compared to the model without mortality (i.e. for $a = 0$) studied in [7] are highlighted. Among the differences that attract attention, on the one hand, we have the operating diagram with different mortality which presents many more cases than the diagram without mortality where it is reduced to only two cases. Thus, the presence of the four regions of stability on the same diagram is now possible. On the other hand, we have the biogas production of the serial device in its maximum state which can be significantly larger than the largest biogas production of the single chemostat. This never happens in the case without mortality. Finally, unlike the case without mortality, the biomass productivity and the biogas flow rate at steady state are not given by the same formulas. Therefore, if biomass productivity is taken into account as a performance criterion, the comparison between the serial chemostat and the single chemostat does not lead to the same conclusions. For more details on this issue the reader can refer to [8].

Appendix

A   The single chemostat

In this section, we give a brief presentation of the mathematical model of the single chemostat with mortality rate. The mathematical equations are given by
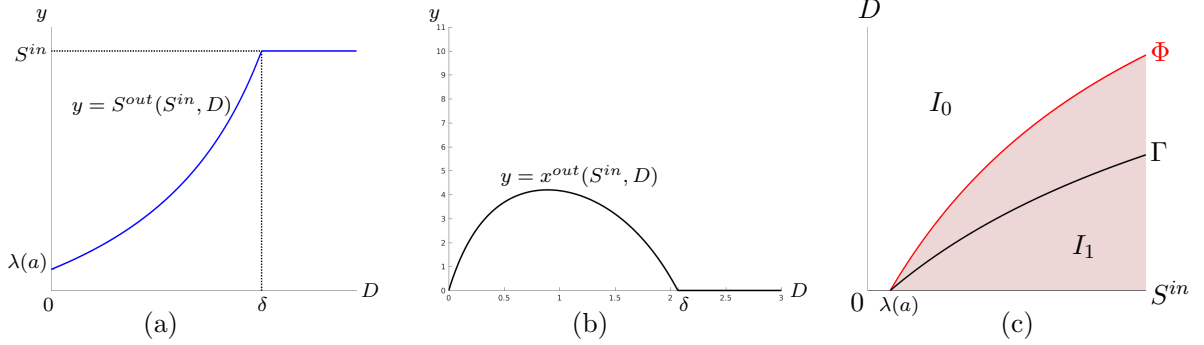

Figure 11: (a) The map $D \mapsto S^{out}(S^{in}, D)$ is increasing on $[0, \delta]$, where $\delta = f(S^{in}) - a$. (b) The map $D \mapsto x^{out}(S^{in}, D)$ with $f(S) = 4S/(5 + S)$, $S^{in} = 10$ and $a = 0.6$. (c) The curve Γ in the operating plane (S^{in}, D) of the single chemostat.

$$\begin{aligned} \dot{S} &= D(S^{in} - S) - f(S)x, \\ \dot{x} &= -Dx + f(S)x - ax, \end{aligned} \tag{50}$$

where S and x denote respectively the substrate and the biomass concentration, S^{in} the input substrate concentration, a the mortality rate and $D = Q/V$ the dilution rate, with Q the input flow rate and V the volume of the tank. The specific growth rate f of the microorganisms satisfies Assumption 1. It is well known (see [16, 38]) that, besides the washout $F_0 = (S^{in}, 0)$, this system can have a positive steady state

$$F_1 = (S^*(D), x^*(S^{in}, D)),$$

where

$$S^* = \lambda(D + a) \quad \text{and} \quad x^* = \frac{D}{D+a}(S^{in} - \lambda(D + a)).$$

See Fig. 11(a) for the plot of the function $D \mapsto S^*(D)$ and Fig. 11(b) for the plot of the function $D \mapsto x^*(S^{in}, D)$ for $0 \leq D \leq \delta$, where $\delta = f(S^{in}) - a$.

The washout steady state F_0 always exists. It is GAS if and only if $D \geq \delta$. It is LES if and only if $D > \delta$. The positive steady state F_1 exists if and only if $D < \delta$. It is GAS and LES whenever it exists. Therefore, the curve Φ defined by

$$\Phi := \{(S^{in}, D) : D = f(S^{in}) - a\} \tag{51}$$

splits the set of operating parameters (S^{in}, D) into two regions, denoted I_0 and I_1, as depicted in 11(c). These regions are defined by

$$\begin{aligned} I_0 &:= \{(S^{in}, D) : D \geq f(S^{in}) - a\}, \\ I_1 &:= \{(S^{in}, D) : D < f(S^{in}) - a\}. \end{aligned} \tag{52}$$

The behavior of the system in each region is given in Table 2. Figure 11(c), together with 2 is called the operating diagram of the single chemostat.

The particularity of this operating diagram is that the curve limiting both regions I_0 and I_1 is translated from zero, unlike the case with mortality, as shown in Figure 2.5 of [16]. Thus, with presence of mortality rate, the region where the washout is GAS, is larger.

Table 2: Stability of steady states in the various regions of the operating diagram.

	I_0	I_1
F_0	GAS	U
F_1		GAS

The output substrate concentration of the single chemostat, at its stable steady state is given by

$$S^{out}(S^{in}, D) = \begin{cases} S^{in} & \text{if} \quad D \geq \delta \\ \lambda(D + a) & \text{if} \quad D < \delta. \end{cases} \tag{53}$$

Its output biomass concentration at steady state is then given by

$$x^{out}(S^{in}, D) = \tfrac{D}{D+a}(S^{in} - S^{out}(D, a)) \tag{54}$$

For all $S^{in} > \lambda(a)$, one has

$$\tfrac{\partial S^{out}}{\partial D}(S^{in}, D) = \begin{cases} 0 & \text{if} \quad D > \delta \\ \lambda'(D + a) & \text{if} \quad D < \delta, \end{cases}$$

Thus, for any growth function satisfying Assumption 1 the function $D \mapsto S^{out}(S^{in}, D)$ is increasing on $[0, \delta]$, as shown in Figure 11(a). The function $D \mapsto x^{out}(S^{in}, D)$ is illustrated in Figure 11(b) for a Monod function.

The biogas flow rate of the single chemostat is defined, up to a multiplicative yield coefficient, by

$$G_{chem}(S^{in}, D) := V x^{out} f(S^{out}). \tag{55}$$

Using the expressions (53) and (54) respectively of S^{out} and x^{out}, the biogas flow rate of the single chemostat is given by:

$$G_{chem}(S^{in}, D) = \begin{cases} 0 & \text{if} \quad D \geq \delta \\ V D(S^{in} - \lambda(D + a)) & \text{if} \quad D < \delta. \end{cases} \tag{56}$$

For a given $S^{in} > \lambda(a)$, the function $D \mapsto G_{chem}(S^{in}, D)$ is null for $D = 0$ or $D \geq \delta$, and is positive for $D \in (0, \delta)$. Therefore it admits a maximum in $(0, \delta)$, which is assumed to be unique. A characterization of the growth functions for which this uniqueness is satisfied can be found in [30].

Proposition 9. *Assume that for any $S^{in} > \lambda(a)$, the maximum of $D \mapsto G_{chem}(S^{in}, D)$ is unique, and define $\overline{D}(S^{in}) \in (0, \delta)$, such that*

$$G_{chem}\left(S^{in}, \overline{D}\left(S^{in}\right)\right) = \max_{D \geq 0} G_{chem}\left(S^{in}, D\right).$$

Then, the dilution rate $D = \overline{D}\left(S^{in}\right)$ is the solution of the equation $S^{in} = g(D)$, where the function $g : [0, m - a) \mapsto \mathbb{R}$ is given by

$$g(D) := \lambda(D + a) + D\lambda'(D + a)). \tag{57}$$

Proof. For any $S^{in} > \lambda(a)$ and $D \in (0, \delta)$, we have

$$\tfrac{\partial G_{chem}}{\partial D}(S^{in}, D) = V\left(S^{in} - \lambda(D + a) - D\lambda'(D + a)\right) \tag{58}$$

Therefore, $\tfrac{\partial G_{chem}}{\partial D}(S^{in}, D) = 0$ if and only if $S^{in} = g(D)$, where g is defined by (57). $\qquad \square$

Notice that the function g defined by (57) is the same as the function g, defined by (19), which was obtained as the limit, when r tends to 1, to the function g_r, defined by (9). Recall that Γ is the curve of equation $S^{in} = g(D)$, see (22). This curve is depicted in Fig. 11(c). It is the set of operating conditions given the higher biogas of the single chemostat. More precisely, for any $S^{in} > \lambda(a)$, the maximum $D = \overline{D}(S^{in})$ of the biogas satisfies the condition $(S^{in}, D) \in \Gamma$. Therefore, a sufficient condition for the uniqueness of $\overline{D}(S^{in})$ is that the mapping g is increasing. If, in addition, f is $\mathcal{C}^2$, then, deriving (58) with respect of D, we have

$$\frac{\partial^2 G_{chem}}{\partial D^2}(S^{in}, D) = -Vg'(D).$$

Hence, a sufficient condition for Assumption 4 to be satisfied is that $g'(D) > 0$ for $D \in [0, m-a)$. This last condition if satisfied whenever $f'' \leq 0$ on $(\lambda(a), +\infty)$, or $\left(\frac{1}{f-a}\right)'' > 0$ on $(\lambda(a), +\infty)$, see Lemma 1 in [30]. Therefore we can make the following remark.

Remark 3. *Linear and Monod growth functions satisfy Assumption 4, since they satisfy $f'' \leq 0$ on $(0, +\infty)$. On the other hand the Hill function satisfy Assumption 4, since it satisfies $\left(\frac{1}{f-a}\right)'' > 0$ on $(\lambda(a), +\infty)$, as shown in Proposition 8.*

B   The serial configuration

We consider a slight extension of system 59 with different mortality rates in the two tanks. Indeed, we assume that the growth environment differs from one tank to another one. This can lead to two different mortality rates in the tanks. We denote by a_1 and a_2 the mortality rates. The mathematical model is given by the following equations.

$$
\begin{aligned}
\dot{S}_1 &= \tfrac{D}{r}(S^{in} - S_1) - f(S_1)x_1 \\
\dot{x}_1 &= -\tfrac{D}{r}x_1 + f(S_1)x_1 - a_1 x_1 \\
\dot{S}_2 &= \tfrac{D}{1-r}(S_1 - S_2) - f(S_2)x_2 \\
\dot{x}_2 &= \tfrac{D}{1-r}(x_1 - x_2) + f(S_2)x_2 - a_2 x_2.
\end{aligned}
\tag{59}
$$

The following result is classical in the mathematical theory of the chemostat.

Lemma 7. *For any nonnegative initial condition, the solution of system* (59) $(S_1(t), x_1(t), S_2(t), x_2(t))$ *is nonnegative for any $t > 0$ and positively bounded.*

Proof. Since the vector field defined by (59) is C^1, the uniqueness of the solution to an initial value problem holds. From (59) and using $f(0) = 0$, we have:

$$
\begin{aligned}
\text{for } i = 1, 2, \quad S_i = 0 &\implies \dot{S}_i > 0, \\
x_1 = 0 &\implies \dot{x}_1 = 0 \\
x_1 \geq 0 \text{ and } x_2 = 0 &\implies \dot{x}_2 \geq 0
\end{aligned}
$$

Therefore, for $i = 1, 2$, $S_i(t) \geq 0$ and $x_i(t) \geq 0$, for all $t \geq 0$, for which they ar defined, provided $S_i(0) \geq 0$ and $x_i(0) \geq 0$, for $i = 1, 2$, see Prop. B.7 in [38]. This proves that the solutions of nonnegative initial conditions are always nonnegative. Let $z_i = S_i + x_i$, $i = 1, 2$. From system (59), we have

$$\dot{z}_1 = \tfrac{D}{r}(S^{in} - z_1) - a_1 x_1, \quad \dot{z}_2 = \tfrac{D}{1-r}(z_1 - z_2) - a_2 x_2.$$

Consequently, we have the differential inequality

$$\dot{z}_1 \leq \tfrac{D}{r}(S^{in} - z_1),$$

It follows by comparison that

$$z_1(t) \leq S^{in} + (z_1(0) - S^{in})e^{-\frac{D}{r}t}$$

Therefore, $z_1(t) \leq Z_1$, where $Z_1 = \max(S^{in}, z_1(0))$. Then, we also have the differential inequality

$$\dot{z}_2 \leq \tfrac{D}{1-r}(Z_1 - z_2).$$

It follows by comparison that

$$z_2(t) \leq Z_1 + (z_2(0) - Z_1)e^{-\frac{D}{1-r}t}$$

Therefore, $z_2(t) \leq Z_2$, where $Z_2 = \max(Z_1, z_2(0))$. Hence, the solutions of (59) are positively bounded. Therefore, they are defined for all $t \geq 0$. $\qquad\square$

For the description of the steady states, we need to define the auxiliary function h given by:

$$h(S_2) = \tfrac{D+(1-r)a_2}{1-r} \tfrac{S_1^* - S_2}{b - S_2},$$

$$\text{where } S_1^* = \lambda\left(\tfrac{D}{r} + a_1\right), \ b = \tfrac{D(S^{in} - S_1^*)}{D + ra_1} + S_1^*. \tag{60}$$

This function satisfies the following property.

Lemma 8. *Assume that $D/r + a_1 < f(S^{in})$. The function h is decreasing from $h(0) > 0$ to $h(S_1^*) = 0$, where $h(0)$ is given by*

$$h(0) = \tfrac{D+(1-r)a_2}{1-r} \tfrac{(D+ra_1)S_1^*}{DS^{in} + ra_1 S_1^*}. \tag{61}$$

Proof. From the condition $D/r + a_1 < f(S^{in})$ it is deduced that $S_1^* < S^{in}$. Note that

$$b = \tfrac{DS^{in} + ra_1 S_1^*}{D + ra_1}.$$

Hence, b is a convex combination of S^{in} and S_1^*, and we have $S_1^* < b < S^{in}$. Therefore, the vertical asymptote $S_2 = b$ of h is at right of S_1^*. The derivative of h is

$$h'(S_2) = \tfrac{D+(1-r)a_2}{1-r} \tfrac{S_1^* - b}{(b - S_2)^2}.$$

Hence, we have $h'(S_2) < 0$ for all $S_2 < b$. Therefore, h is defined on the interval $(0, S_1^*)$ and is decreasing from $h(0)$, given by (61) to $h(S_1^*) = 0$. $\qquad\square$

Therefore, if $D/r + a_1 < f(S^{in})$, equation $f(S_2) = h(S_2)$ admits a unique solution, denoted by $S_2^*(S^{in}, D, r)$, as shown in Fig. 12(a). This solution satisfy the following property.

Lemma 9. *For all $0 \leq D < f(S^{in}) - a$, one has*

$$\lim_{r \to 1} S_2^*(S^{in}, D, r) = \lambda(D + a).$$

Proof. Let $0 \leq D < f(S^{in}) - a$. Using (5), the condition $h(S_2) = f(S_2)$ is equivalent to

$$(D + (1-r)a)(S_1^* - S_2^*) =$$
$$(1-r)\left(\tfrac{D}{D+ra}(S^{in} - S_1^*) + S_1^* - S_2^*\right)f(S_2^*). \tag{62}$$

As $S_1^*|_{r=1} = \lambda(D + a)$ and $\lim_{r \to 1} f(S_2^*) < +\infty$ then, (62) gives

$$D(\lambda(D + a) - \lim_{r \to 1} S_2^*(S^{in}, D, r)) = 0.$$

Consequently, one has $\lim_{r \to 1} S_2^*(S^{in}, D, r)) = \lambda(D + a)$. $\qquad\square$

The existence and stability of steady states of (59) are given by the following result.

Theorem 3. *Assume that Assumption 1 is satisfied. The steady states of (59) are:*
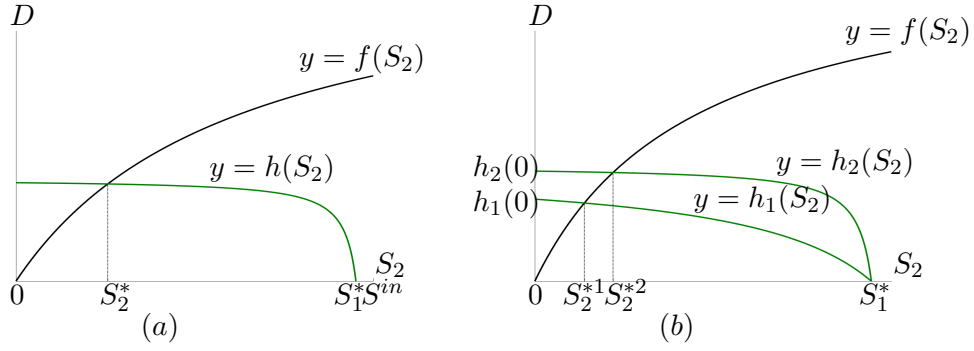
Figure 12: (a) Existence and uniqueness of the solution S_2^* of equation $f(S_2) = h(S_2)$. (b) Graphical illustration of Proposition 10: S_2^* decreases when S^{in} increases.

- *The washout steady state $E_0 = (S^{in}, 0, S^{in}, 0)$ which always exists. It is GAS if and only if*

$$D \geq \max\{r(f(S^{in}) - a_1), (1-r)(f(S^{in}) - a_2)\}. \tag{63}$$

  It is LES if and only if

$$D > \max\{r(f(S^{in}) - a_1), (1-r)(f(S^{in}) - a_2)\}.$$

- *The steady state $E_1 = (S^{in}, 0, \overline{S}_2, \overline{x}_2)$ of washout in the first chemostat but not in the second one with*

$$\overline{S}_2 = \lambda\left(\frac{D}{1-r} + a_2\right), \quad \overline{x}_2 = \frac{D}{D + (1-r)a_2}\left(S^{in} - \overline{S}_2\right). \tag{64}$$

  It exists if and only if $D < (1-r)(f(S^{in}) - a_2)$. It is GAS if and only if

$$r(f(S^{in}) - a_1) \leq D \text{ and } D < (1-r)(f(S^{in}) - a_2). \tag{65}$$

  It is LES if and only if

$$r(f(S^{in}) - a_1) < D < (1-r)(f(S^{in}) - a_2).$$

- *The steady state $E_2 = (S_1^*, x_1^*, S_2^*, x_2^*)$ of persistence of the species in both chemostats with*

$$S_1^* = \lambda\left(\frac{D}{r} + a_1\right), \quad x_1^* = \frac{D}{D + ra_1}(S^{in} - S_1^*), \tag{66}$$

$$x_2^* = \frac{D}{D + (1-r)a_2}\left(\frac{D}{D + ra_1}(S^{in} - S_1^*) + S_1^* - S_2^*\right) \tag{67}$$

  and $S_2^* = S_2^*(S^{in}, D, r)$ is the unique solution of the equation $h(S_2) = f(S_2)$ with h defined by (60). This steady state exists and is positive if and only if $D < r(f(S^{in}) - a_1)$. It is GAS and LES whenever it exists and is positive.

Proof. The 4-dimensional system of ODEs (59) has a cascade structure of two planar systems of ODEs, whose mathematical analysis is easy and well known in the mathematical theory of the chemostat [16, 38]. Using this cascade structure, the global behavior of the system is deduced from the global behaviour of planar systems and Thieme's theory of asymptotically autonomous systems.

For the convenience of the reader the details of the proof are given in Appendix D.1. □

Proposition 10. *The function $S^{in} \mapsto S_2^*(S^{in}, D, r)$ is decreasing.*

Proof. D and r are fixed. Let $S^{in,1} > S^{in,2}$ and h_i defined by (60), with $S^{in} = S^{in,i}$, $i = 1, 2$. Let S_2^{*i}, the solution of equation $f(S_2) = h_i(S_2)$, $i = 1, 2$. Using Lemma 8, h_i is a decreasing hyperbola from $h_i(0)$ defined by (61), with $S^{in} = S^{in,i}$, to $h_i(S_1^*) = 0$. Since $h_1(0) < h_2(0)$, we have $h_1(S_2) < h_2(S_2)$ for all $S_2 \in (0, S_1^*)$. Therefore, $S_2^{*1} < S_2^{*2}$, see Fig. 12(b). □

This result means that the effluent steady state concentration of substrate decreases when the influent concentration of substrate increases. This behavior is very different from the single chemostat, where the effluent steady state substrate concentration is independent of the influent substrate concentration.
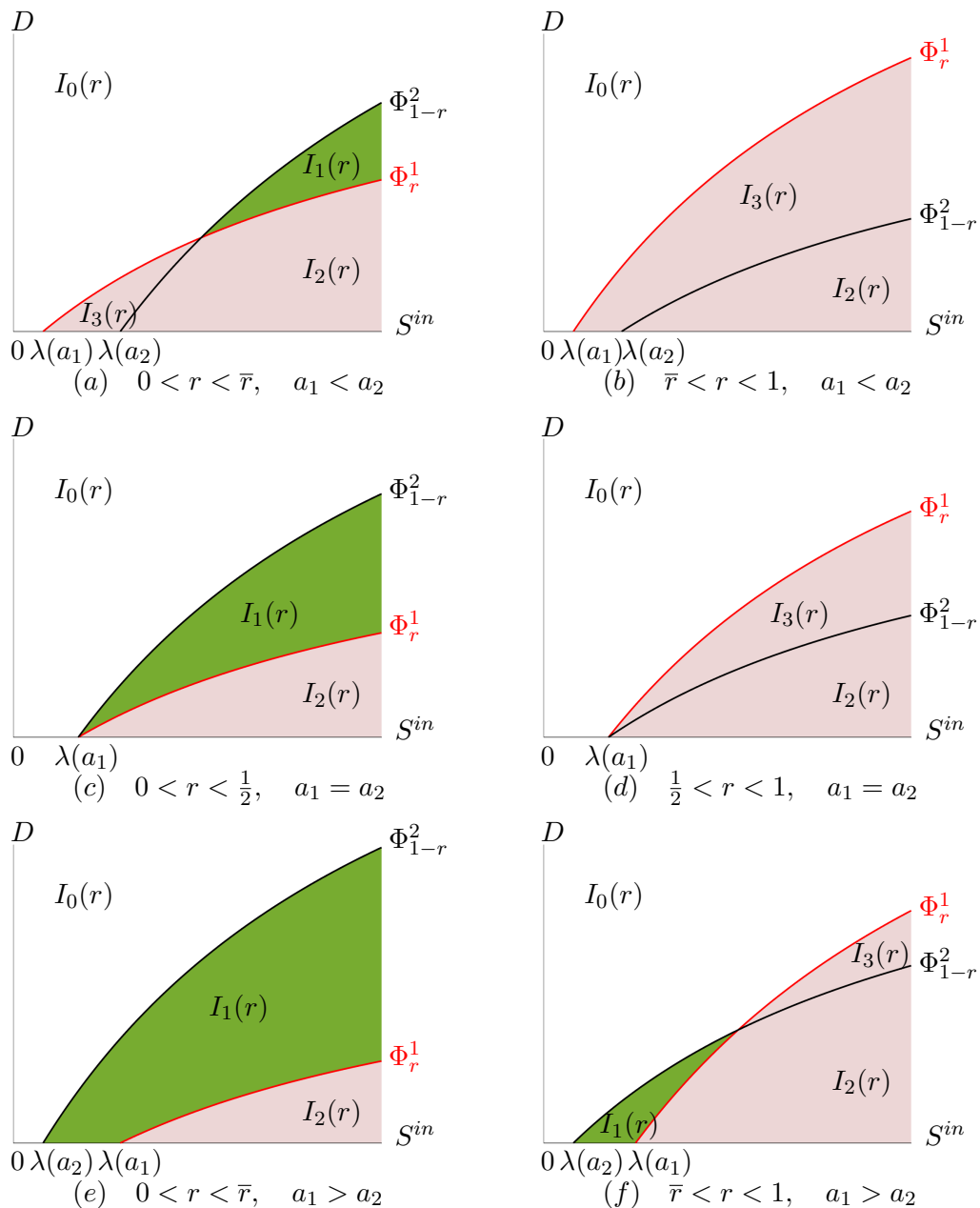
Figure 13: The operating diagram of (59). The asymptotic behaviour in each region is depicted in Table 3.

C   Operating diagram

For the chemostat model, the operating diagram has as coordinates the input substrate concentration S^{in} and the dilution rate D, and shows how the solutions of the system behave for different values of these two parameters. The regions constituting the operating diagram correspond to different qualitative asymptotic behaviors. Indeed, the main interest of an operating diagram is to highlight the number and stability of the steady states for a given pair of parameters (S^{in}, D). The input substrate concentration S^{in} and the dilution rate D are the usual

Table 3: The regions $I_k(r)$, $k = 0, 1, 2, 3$ of the operating diagram of (59) and asymptotic behaviour in these various regions.

Regions
$I_0(r) = \left\{(S^{in}, D) : \max\{r(f(S^{in}) - a_1), (1 - r)(f(S^{in}) - a_2)\} \leq D\right\}$
$I_1(r) = \left\{(S^{in}, D) : r(f(S^{in}) - a_1) \leq D \text{ and } D < (1 - r)(f(S^{in}) - a_2)\right\},$
$I_2(r) = \left\{(S^{in}, D) : 0 < D < \min\{r(f(S^{in}) - a_1), (1 - r)(f(S^{in}) - a_2)\}\right\},$
$I_3(r) = \left\{(S^{in}, D) : (1 - r)(f(S^{in}) - a_2) \leq D \text{ and } D < r(f(S^{in}) - a_1)\right\}.$

	$I_0(r)$	$I_1(r)$	$I_2(r)$	$I_3(r)$
E_0	GAS	U	U	U
E_1		GAS	U	
E_2			GAS	GAS

parameters manipulated by the experimenter of a chemostat. Apart from these parameters, and the parameter r that can be also chosen by the experimenter but not easily changed as S^{in} and D, all other parameters have biological meaning and are fitted using experimental data from real measurements of concentrations of micro-organisms and substrates. Therefore the operating diagram is a bifurcation diagram, quite useful to understand the possible behaviors of the solutions of the system from both the mathematical and biological points of view.

Here, we fix $r \in (0, 1)$ and we depict in the plane (S^{in}, D) the regions in which the solution of system (59) globally converges towards one of the steady state E_0, E_1 or E_2. From the results given in Theorem 3, it is seen that these regions are delimited by the curves Φ_r^1 and Φ_{1-r}^2 defined by:

$$\Phi_r^1 := \left\{(S^{in}, D) \in \mathbb{R}_+^2 : D = r(f(S^{in}) - a_1)\right\}, \tag{68}$$

$$\Phi_{1-r}^2 := \left\{(S^{in}, D) \in \mathbb{R}_+^2 : D = (1 - r)(f(S^{in}) - a_2)\right\}. \tag{69}$$

When $a_1 = a_2 = 0$, as we have shown in [7], these curves meet only at one point (the origin) and merge when $r = 1/2$. Therefore, in this case the curves Φ_r^1 and Φ_{1-r}^2 separate the operating plane (S^{in}, D), in only three regions, see [7, Figure 5]. This property continue to hold when $a_1 = a_2$, that is to say, the curves intersect only at $(\lambda(a_1), 0)$ and merge when $r = 1/2$. In this case the curves Φ_r^1 and Φ_{1-r}^2 separate the operating plane (S^{in}, D), in only three regions, see Figure 13 (c) and (d). The novelty when a_1 and a_2 are different and non null, is that the intersection of the curves Φ_r^1 and Φ_{1-r}^2 can lie outside the S^{in} axis. Therefore there can be four regions in the operating plane, as depicted in Figure 13 (a) and (f). For the description of the intersection of the curves Φ_r^1 and Φ_{1-r}^2, we need some definitions and notations. Let $\overline{r} \in (0, 1)$ be defined by

$$\overline{r} := \frac{m - a_2}{2m - a_1 - a_2}. \tag{70}$$

Note that if $a_1 < a_2$ then $\overline{r} < 1/2$, and if $a_1 > a_2$ then $\overline{r} > 1/2$. For $a_1 < a_2$ and $0 < r < \overline{r}$ (or $a_1 > a_2$ and $\overline{r} < r < 1$), we define the point $P = \left(S_P^{in}, D_P\right)$ of the operating plane by:

$$S_P^{in} := \lambda\left(\frac{ra_1 - (1-r)a_2}{2r - 1}\right), \quad D_P := \frac{r(1-r)(a_2 - a_1)}{1 - 2r}. \tag{71}$$

Note that $S_P^{in} > 0$ and $D_P > 0$. With these notations we can state the following result:

Proposition 11.   *1. If $a_1 < a_2$ then for all $r \in (0, \overline{r})$, the curves Φ_r^1 and Φ_{1-r}^2 intersect at the point P and Φ_r^1 is strictly below [resp. above] Φ_{1-r}^2 for $S^{in} > S_P^{in}$ [resp. $S^{in} < S_P^{in}$], see Figure 13 (a). For all $r \in (\overline{r}, 1)$, Φ_r^1 is strictly above Φ_{1-r}^2, see Figure 13 (b).*

2. If $a_1 > a_2$ then for all $r \in (\overline{r}, 1)$, the curves Φ_r^1 and Φ_{1-r}^2 intersect at the point P and Φ_r^1 is strictly above [resp. below] Φ_{1-r}^2 for $S^{in} > S_P^{in}$ [resp. $S^{in} < S_P^{in}$], see Figure 13 (f). For all $r \in (0, \overline{r})$, Φ_r^1 is below Φ_{1-r}^2, see Figure 13 (e).

3. If $a_1 = a_2$ then, for $r = 1/2$, $\Phi^1_r = \Phi^2_{1-r}$. Moreover, if $r < 1/2$ then Φ^1_r is strictly below Φ^2_{1-r}, see Figure 13 (c) and, if $r > 1/2$ then Φ^1_r is strictly above Φ^2_{1-r}, see Figure 13 (d).

Proof. For $0 < r < 1$ and $S^{in} > \lambda(a_i)$ we define the function φ_i, $i = 1, 2$, by

$$
\begin{aligned}
\varphi_1(S^{in}, r) &= r(f(S^{in}) - a_1), \\
\varphi_2(S^{in}, r) &= (1 - r)(f(S^{in}) - a_2).
\end{aligned}
\tag{72}
$$

The curves Φ^1_r and Φ^2_{1-r}, defined respectively by (68) and (69), intersect if and only if there exists $r \in (0, 1)$ and $S^{in} > \max(\lambda(a_1), \lambda(a_2))$ such that $\varphi_1(S^{in}, r) = \varphi_2(S^{in}, r)$, that is to say

$$
f(S^{in}) = A(r), \quad \text{with} \quad A(r) := \tfrac{ra_1 - (1-r)a_2}{2r - 1}.
\tag{73}
$$

This equation has a solution $S^{in} > \max(\lambda(a_1), \lambda(a_2))$ if and only if

$$
\max(a_1, a_2) < A(r) < m,
\tag{74}
$$

where $m = \sup(f)$, as in (2). When these conditions are satisfied, the solution of (73) is given by $S^{in} = \lambda(A(r))$, where λ is the inverse function pf f, i.e. the break-even concentration defined by (3). Hence, $S^{in} = S^{in}_P$, given in (71). The corresponding intersection point of Φ^1_r and Φ^2_{1-r} is given by $D_P = r\left(f(S^{in}_P) - a_1\right)$, which is the value given in (71).

Let us determine now for which value of r, the conditions (74) are satisfied. The function A is a homographic function. Its graphical representation is a hyperbola, whose vertical asymptote is $r = 1/2$. Its derivative is given by

$$
A'(r) = \frac{a_2 - a_1}{(2r - 1)^2}.
\tag{75}
$$

Note that $A(r) = m$ if and only if $r = \bar{r}$, where $\bar{r}$ is defined by (70). Therefore if $a_1 < a_2$ then, according to (75), A is increasing. Since $A(0) = a_2$, $A(\bar{r}) = m$, and $\bar{r} < 1/2$, the condition (74) is satisfied if and only if $0 < r < \bar{r}$. Similarly, if $a_1 > a_2$, then, according to (75), A is decreasing. Since $A(1) = a_1$, $A(\bar{r}) = m$ and $\bar{r} > 1/2$, the condition (74) is satisfied if and only if $\bar{r} < r < 1$. Finally, if $a_1 = a_2$ then $A(r) = a_1$ and the condition (74) cannot be satisfied.

Suppose that $a_1 < a_2$. Note that for $0 < r < 1/2$, the condition $f(S^{in}) > A(r)$ [resp. $f(S^{in}) < A(r)$] is equivalent to $\varphi_1(S^{in}, r) < \varphi_2(S^{in}, r)$ [resp. $\varphi_1(S^{in}, r) > \varphi_2(S^{in}, r)$]. Thus:

- If $r \in (0, \bar{r})$, then $f(S^{in}) < A(r)$ if and only if $S^{in} < S^{in}_P$, where S^{in}_P is defined by (71). Hence, the curves Φ^1_r and Φ^2_{1-r} intersect at $P = (S^{in}_P, D_P)$ and the curve Φ^1_r is strictly below [resp. above] the curve Φ^2_{1-r}, for all $S^{in} > S^{in}_P$ [resp. $S^{in} < S^{in}_P$].

- If $r \in [\bar{r}, 1/2)$ then $f(S^{in}) < A(r)$ for all $S^{in} > 0$, so that the curve Φ^1_r is strictly above the curve Φ^2_{1-r}.

- If $r \in [1/2, 1)$, then, using $r \geq 1 - r$ and $a_1 < a_2$, one has $\varphi_1(S^{in}, r) > \varphi_2(S^{in}, r)$. Therefore, the curve Φ^1_r is strictly above the curve Φ^2_{1-r}.

If $a_1 > a_2$, the proof is similar to the case $a_1 < a_2$.

If $a_1 = a_2$ then $\varphi_1(S^{in}, r) = \varphi_2(S^{in}, r)$ is equivalent to $r(f(S^{in}) - a_1) = (1 - r)(f(S^{in}) - a_1)$. Therefore, $r = 1 - r$, that is $r = 1/2$. In this case the curves Φ^1_r and Φ^2_{1-r} merge. In addition, if $r < 1/2$ [resp. $r > 1/2$] then $r < 1 - r$ [resp. $r > 1 - r$] and the curve Φ^1_r is strictly below [resp. above] the curve Φ^2_{1-r}. This ends the proof of the proposition. $\qquad\square$

For any $r \in (0, 1)$, the curves Φ^1_r and Φ^2_{1-r}, defined by (68) and (69), respectively split the plane (S^{in}, D) in the regions denoted $I_0(r)$, $I_1(r)$, $I_2(r)$ and $I_3(r)$ and defined in Table 3. These regions are depicted in Fig. 13 in the cases $a_1 < a_2$, $a_1 = a_2$ and $a_1 > a_2$.

The behavior of the system in each region, when it is not empty, is given in Table 3. Notice that E_1 exists in both regions $I_1(r)$ and $I_2(r)$, but is stable only when (S^{in}, D) is fixed in $I_1(r)$.

When $a_1 = a_2 = 0$ then $\lambda(a_1) = \lambda(a_2) = 0$ and the curves Φ^1_r and Φ^2_{1-r} of the operating diagram start from the origin of the plane (S^{in}, D) and merge for $r = 1/2$. Therefore, the

diagrams shown in panels (a), (b), (c), (d), (e) and (f) of Fig. 13 are reduced to only two different cases characterized by $0 < r < 1/2$ and $1/2 < r < 1$, as shown in Figure 5 of [7]. There is no changes in the stability of the steady states and in the number of the regions depicted in the operating diagram.

This result reveals an interplay between spatial heterogeneity (the ratio r of volume distribution between tanks) and the mortality heterogeneity (difference between a_1 and a_2). Indeed, panels (a) and (f) of Fig. 13 bring a particular feature when mortality rates are different: domains $I_1(r)$ and $I_3(r)$ can appear or disappear playing only with the spatial distribution r, a phenomenon which does not happens when mortality is identical in each tank. This shows that the existence of domains $I_1(r)$ and $I_3(r)$ is controlled by a relative toxicity in the tanks, and not only the spatial distribution as it is the case for identical mortality. This feature can have interest when practitioners can adjust pH or other abiotic parameters having impacts on the mortality rate, independently in each tank. Given operating parameters S^{in}, D and r, panels (a) and (f) of Fig. 13 show that it is theoretically possible to pass from domain $I_3(r)$ to $I_2(r)$ when mortality parameter is diminished only in the second tank. In practice, being in domain $I_2(r)$ might be more desirable than $I_3(r)$ with respect to some dysfunctioning of the first tank that can drop suddenly its biomass to zero. Indeed, in $I_2(r)$, the second tank is no conducted to the wash-out differently to the $I_3(r)$ case.

When $a_1 = a_2 = a$, which is the case corresponding to the system (1) considered in Section 2, only panels (c,d) of Fig. 13 are encountered, as shown in Fig. 2. We describe hereafter the bifurcations that occur in this particular case. The general case i.e. when $a_1 \neq a_2$ is similar.

Remark 4. *Transcritical bifurcations occur in the limit cases $D = r(f(S^{in}) - a)$ and $D = (1-r)(f(S^{in}) - a)$, for system (1). If $0 < r < 1/2$ then, we have a transcritical bifurcation of E_0 and E_1 when $D = (1-r)(f(S^{in}) - a)$ and a transcritical bifurcation of E_1 and E_2 when $D = r(f(S^{in}) - a)$. If $1/2 < r < 1$ then, we have a transcritical bifurcation of E_0 and E_1 when $D = (1-r)(f(S^{in}) - a)$ and a transcritical bifurcation of E_0 and E_2 when $D = r(f(S^{in}) - a)$. If $r = 1/2$ and $D = (f(S^{in}) - a)/2$ then, we have transcritical bifurcations of E_0 and E_1, and E_0 and E_2, simultaneously.*

D   Proofs

D.1   Proof of Theorem 3

We begin by the existence of steady states. The steady states are the solutions of the set of equations $\dot{S}_1 = 0$, $\dot{x}_1 = 0$, $\dot{S}_2 = 0$, $\dot{x}_2 = 0$. From equation $\dot{x}_1 = 0$, it is deduced that $x_1 = 0$ or $f(S_1) = D/r + a_1$. Suppose first that $x_1 = 0$. Then, from equation $\dot{S}_1 = 0$ it is deduced that $S_1 = S^{in}$ and from equation $\dot{x}_2 = 0$ it is deduced that $x_2 = 0$ or $f(S_2) = D/(1-r) + a_2$. If $x_2 = 0$, then from equation $\dot{S}_2 = 0$ it is deduced that $S_2 = S^{in}$. Hence we obtain the steady state $E_0 = (S^{in}, 0, S^{in}, 0)$, which always exist. On the other hand, if $f(S_2) = D/(1-r) + a_2$, then $S_2 = \overline{S}_2$, defined in (64). From equation $\dot{S}_2 = 0$, it is deduced that $x_2 = \overline{x}_2$, defined in (64). Hence we obtain the steady state $E_1 = (S^{in}, 0, \overline{S}_2, \overline{x}_2)$. This steady state exists if and only if $S^{in} > \overline{S}_2$, that is $D < (1-r)(f(S^{in}) - a_2)$.

Suppose now that $f(S_1) = D/r + a_1$. Then $S_1 = S_1^*$, defined in (66). From equation $\dot{S}_1 = 0$, it is deduced that $x_1 = x_1^*$, defined in (66). From equation $\dot{S}_2 + \dot{x}_2 = 0$, it is deduced that

$$x_2 = \frac{D}{D + (1-r)a_2}(S_1^* + x_1^* - S_2). \tag{76}$$

Replacing x_2 by this expression in the equation $\dot{S}_2 = 0$, it is deduced that $f(S_2) = h(S_2)$, where h is defined by (60). Hence $S_2 = S_2^*$, which is the unique solution of the equation $f(S_2) = h(S_2)$, as shown in Figure 12 (a). Replacing S_2 by S_2^* in (76) gives $x_2 = x_2^*$, defined by (67). Consequently, we obtain the steady state $E_2 = (S_1^*, x_1^*, S_2^*, x_2^*)$. This steady state is positive if and only if $S^{in} > S_1^*$, which is equivalent to $D < r(f(S^{in}) - a_1)$.

Let us now study the local stability. Since the system has a cascade structure, the stability analysis reduces to the study of square 2×2 matrices. Indeed, the Jacobian matrix associated to system (59) is the lower triangular matrix by blocs, $J = \begin{pmatrix} A & 0 \\ B & C \end{pmatrix}$ where B is the diagonal matrix whose diagonal elements are $D/(1-r)$, and A and C are given by:

$$A = \begin{pmatrix} -\frac{D}{r} - f'(S_1)x_1 & -f(S_1) \\ f'(S_1)x_1 & -\frac{D}{r} + f(S_1) - a_1 \end{pmatrix},$$
$$C = \begin{pmatrix} -\frac{D}{1-r} - f'(S_2)x_2 & -f(S_2) \\ f'(S_2)x_2 & -\frac{D}{1-r} + f(S_2) - a_2 \end{pmatrix},$$

Hence, the eigenvalues of J are the ones of A and C.

For E_0, the eigenvalues are $-D/r$, $-D/r + f(S^{in}) - a_1$, $-D/(1-r)$ and $-D/(1-r) + f(S^{in}) - a_2$. They are negative if and only if $D > r(f(S^{in}) - a_1)$ and $D > (1-r)(f(S^{in}) - a_2)$. Therefore, E_0 is LES if and only if the condition in the theorem is satisfied.

For E_1, the eigenvalues of A are $-D/r + f(S^{in}) - a_1$ and $-D/r$. The first eigenvalue is negative if and only if $D > r(f(S^{in}) - a_1)$. On the other hand, since the determinant of C is positive, and its trace is negative, the eigenvalues of C are of negative real parts. Therefore, E_1 is LES if and only if the condition in the theorem is satisfied.

For E_2, the determinant of A is positive and its trace is negative. On the other hand, using the notation C_{E_2} for the matrix C evaluated at E_2, we have

$$\begin{aligned} \det(C_{E_2}) &= \left(-\frac{D}{1-r} - f'(S_2^*)x_2^*\right)\left(-\frac{D}{1-r} - a_2 + f(S_2^*)\right) + f(S_2^*)f'(S_2^*)x_2^*, \\ \operatorname{tr}(C_{E_2}) &= -2\frac{D}{1-r} - a_2 - f'(S_2^*)x_2^* + f(S_2^*). \end{aligned}$$

Note that $h(S_2) < D/(1-r) + a_2$ for all $S_2 \in (0, S_1^*)$. Therefore, from (60), we have $f(S_2^*) = h(S_2^*) < D/(1-r) + a_2$. Consequently, $\det(C_{E_2})$ and $\operatorname{tr}(C_{E_2})$ are respectively positive and negative. Therefore, E_2 is LES whenever it exists, that is $D < r(f(S^{in}) - a_1)$.

For the study of the global stability we use the cascade structure of the system (59) and Thieme's Theorem (see Theorem A1.9 of [16]). In the rest of the proof, we denote by $(S_1(t), x_1(t), S_2(t), x_2(t))$ the solution of (59) with the initial condition $(S_1^0, x_1^0, S_2^0, x_2^0)$. Then, $(S_1(t), x_1(t))$ is the solution of system

$$\begin{aligned} \dot{S}_1 &= \frac{D}{r}(S^{in} - S_1) - f(S_1)x_1 \\ \dot{x}_1 &= -\frac{D}{r}x_1 + f(S_1)x_1 - a_1 x_1 \end{aligned} \tag{77}$$

with initial condition (S_1^0, x_1^0) and $(S_2(t), x_2(t))$ is the solution of the non-autonomous system of differential equations

$$\begin{aligned} \dot{S}_2 &= \frac{D}{1-r}(S_1(t) - S_2) - f(S_2)x_2 \\ \dot{x}_2 &= \frac{D}{1-r}(x_1(t) - x_2) + f(S_2)x_2 - a_2 x_2 \end{aligned} \tag{78}$$

with the initial condition (S_2^0, x_2^0). The system (77) is the classical model of a single chemostat. Its asymptotic behaviour is well known (see, for instance, Proposition 2.2 of [16]). This system admits the steady states:

$$e_0^1 = \left(S^{in}, 0\right) \quad \text{and} \quad e_1^1 = (S_1^*, x_1^*) \tag{79}$$

where S_1^* and x_1^* are defined by (66). Two cases must be distinguished.

Firstly, if $\lambda(D/r + a_1) \geq S^{in}$, that is $D \geq r(f(S^{in}) - a_1)$ then, e_0^1, defined in (79), is GAS for (77) in the nonnegative quadrant. Hence, for any non-negative initial condition (S_1^0, x_1^0),

$$\lim_{t \to +\infty}(S_1(t), x_1(t)) = (S^{in}, 0). \tag{80}$$

Therefore, the system (78) is asymptotically autonomous with the limiting system

$$\begin{array}{rcl}
\dot{S}_2 & = & \frac{D}{1-r}(S^{in} - S_2) - f(S_2)x_2 \\
\dot{x}_2 & = & -\frac{D}{1-r}x_2 + f(S_2)x_2 - a_2 x_2.
\end{array} \qquad (81)$$

Recall that the solutions of (78) are positively bounded. Therefore, we shall use Thieme's results which apply for bounded solutions.

The system (81) represents the classical model of a single chemostat. It admits the two steady states $e_0^2 = (S^{in}, 0)$ and $e_1^2 = (\overline{S}_2, \overline{x}_2)$, with $(\overline{S}_2, \overline{x}_2)$ defined by (64). Two subcases must be distinguished

- If $\lambda\left(D/(1-r) + a_2\right) \geq S^{in}$, that is $D \geq (1-r)(f(S^{in}) - a_2)$ then, e_0^2 is GAS in the nonnegative quadrant. Using Thieme's Theorem, we deduce that for any nonnegative (S_2^0, x_2^0), the solution $(S_2(t), x_2(t))$ of (78) converges towards $e_0^2 = (S^{in}, 0)$. Using (80) we deduce that, when $D \geq \max(r(f(S^{in}) - a_1), (1-r)(f(S^{in}) - a_2))$, the solution $(S_1(t), x_1(t), S_2(t), x_2(t))$ of (59) converges towards $E_0 = (S^{in}, 0, S^{in}, 0)$, which proves (63).

- In contrast, if $\lambda(D/(1-r) + a_2) < S^{in}$, that is $D < (1-r)(f(S^{in}) - a_2)$ then, both steady states e_0^2 and e_1^2 exist and e_1^2 is GAS in the positive quadrant. Although system (78) has the saddle point e_0^2, no polycycle can exist. Using Thieme's Theorem, for any positive (S_2^0, x_2^0), the solution $(S_2(t), x_2(t))$ of (78) converges towards $e_1^2 = (\overline{S}_2, \overline{x}_2)$. Using (80) we deduce that, if $r(f(S^{in}) - a_1) \leq D$ and $D < (1-r)(f(S^{in}) - a_2)$, then the solution $(S_1(t), x_1(t), S_2(t), x_2(t))$ of (59) converges towards $E_1 = \left(S^{in}, 0, \overline{S}_2, \overline{x}_2\right)$, which proves (65).

Secondly, if $\lambda\left(D/r + a_1\right) < S^{in}$, that is $D < r(f(S^{in}) - a_1)$ then, e_1^1, defined in (79), is GAS for (77) in the positive quadrant. Hence, for any positive initial condition (S_1^0, x_1^0)

$$\lim_{t \to +\infty} (S_1(t), x_1(t)) = (S_1^*, x_1^*). \qquad (82)$$

Therefore, the system (78) is asymptotically autonomous with the limiting system

$$\begin{array}{rcl}
\dot{S}_2 & = & \frac{D}{1-r}(S_1^* - S_2) - f(S_2)x_2 \\
\dot{x}_2 & = & \frac{D}{1-r}(x_1^* - x_2) + f(S_2)x_2 - a_2 x_2.
\end{array} \qquad (83)$$

The system (83) represents the classical model of a single chemostat with an input biomass. In this case, there is no washout and the system (83) always admits one LES steady state $e_2 = (S_2^*, x_2^*)$ with positive biomass defined by (67) and S_2^* the unique solution of $h(S_2) = f(S_2)$.

Let us show that this steady state is GAS for (83). Assume that $x_2 > 0$. Consider the change of variable $\xi = \ln(x_2)$. The system (83) becomes as

$$\begin{array}{rcl}
\dot{S}_2 & = & \frac{D}{1-r}(S_1^* - S_2) - f(S_2)e^\xi \\
\dot{\xi} & = & \frac{D}{1-r}(x_1^* e^{-\xi} - 1) + f(S_2) - a_2.
\end{array} \qquad (84)$$

The divergence of the vector field

$$\psi(S_2, \xi) = \left[\begin{array}{c}
\frac{D}{1-r}(S_1^* - S_2) - f(S_2)e^\xi \\
\frac{D}{1-r}(x_1^* e^{-\xi} - 1) + f(S_2) - a_2
\end{array} \right]$$

associated to (84) is $\text{div}\psi(S_2, \xi) = -\frac{D}{1-r}(1 + x_1^* e^\xi) - f'(S_2)e^\xi$. It is negative. Thus, using Bendixon-Dulac criterion, system (84) cannot have a periodic solution. Hence, system (83) has no cycle in the positive quadrant. For any non negative initial condition (S_2^0, x_2^0), the solution of (83) is bounded. Hence, the ω-limit set of (S_2^0, x_2^0), denoted $\omega(S_2^0, x_2^0)$, is non-empty and included in the positive quadrant. If $e_2 \notin \omega(S_2^0, x_2^0)$ then, using Poincaré-Bendixon Theorem, $\omega(S_2^0, x_2^0)$ is a limit cycle, but the system does not present any, due to the divergence property. One then deduces $e_2 \in \omega(S_2^0, x_2^0)$ and, as e_2 is LES, then $\omega(S_2^0, x_2^0) = \{e_2\}$. Consequently, e_2 is GAS for (83) in the positive quadrant.

Using again Thieme's Theorem, for any positive (S_2^0, x_2^0), the solution $(S_2(t), x_2(t))$ of (78)

35

converges towards $e_2 = (S_2^*, x_2^*)$. Using (82) we deduce that, if $D < r(f(S^{in}) - a_1)$, then the solution $(S_1(t), x_1(t), S_2(t), x_2(t))$ of (59) converges towards $E_2 = (S_1^*, x_1^*, S_2^*, x_2^*)$. This ends the proof of the theorem.

D.2 Proof of Lemma 4

Let us fix S^{in} such that $\delta := f(S^{in}) - a > 0$. The proof consists in showing that the function $(D, r) \mapsto G_2(S^{in}, D, r)$ can be formally extended as a C^2 function for values of r larger than 1 (although such values have no physical meaning). Recall first that for any $D \in (0, \delta)$, one has $G_2(S^{in}, D, 1) = G_{chem}(S^{in}, D)$. As $G_2(S^{in}, \overline{D}(1), 1) > 0$ and $G_2(S^{in}, 0, 1) = 0$, there exists by continuity of the function G_2, numbers $\underline{D} \in (0, \overline{D}(1))$, $\underline{r} \in (0, 1)$ such that

$$G_2(S^{in}, D, r) < \max_{d \in (0, r\delta)} G_2(S^{in}, d, r), \ (D, r) \in [0, \underline{D}] \times [\underline{r}, 1] \tag{85}$$

Let $\varepsilon > 0$ be such that

$$D_\varepsilon := \epsilon \left(a + \max_{s \in [0, S^{in}]} f'(s)(S^{in} - s) \right) < \underline{D} \tag{86}$$

and consider the domain

$$\mathcal{D}_\varepsilon := \left\{ (D, r); \ D \in (D_\varepsilon, \delta), \ r \in \left(\max\left(\underline{r}, \frac{D}{\delta} \right), 1 + \varepsilon \right) \right\}$$

Note that for any $(D, r) \in \mathcal{D}_\varepsilon$, the number $\lambda(D/r + a) = f^{-1}(D/r + a)$ is well defined. Posit the function

$$\varphi(S_2, D, r) = (D + (1 - r)a)(\lambda(D/r + a) - S_2) - (1 - r)f(S_2)\left(\frac{DS^{in} + ra\lambda(D/r+a)}{D+ra} - S_2 \right),$$

where $(S_2, D, r) \in (0, S^{in}) \times \mathcal{D}_\varepsilon$. As f is C^2, φ is C^2 on $(0, S^{in}) \times \mathcal{D}_\varepsilon$.

For $r < 1$ and $(D, r) \in \mathcal{D}_\varepsilon$, one has

$$\varphi(S_2, D, r) = (1 - r)\left(\frac{DS^{in} + ra\lambda(D/r + a)}{D + ra} - S_2 \right).$$
$$(h(S_2) - f(S_2))$$

where h is the function defined in (5). According to Lemma 8, h is positive decreasing on $(0, \lambda(D/r + a))$, and $h - f$ admits an unique zero $S_2^\star = S_2^\star(S^{in}, D, r)$ on $(0, \lambda(D/r + a))$. Then, one can write

$$\partial_{S_2}\varphi \Big|_{S_2 = S_2^\star} = (1 - r)\left(\frac{DS^{in} + ra\lambda(D/r + a)}{D + ra} - S_2 \right).$$
$$\left(\partial_{S_2}h - f' \right)\Big|_{S_2 = S_2^\star} < 0$$

For $r \in [1, 1 + \varepsilon)$ and $(D, r) \in \mathcal{D}_\varepsilon$, on has

$$\partial_{S_2}\varphi = -(D + (1 - r)a)$$
$$- (1 - r)f'(S_2)\left(\frac{DS^{in} + ra\lambda(D/r + a)}{D + ra} - S_2 \right)$$
$$+ (1 - r)f(S_2),$$

which is negative for any $S_2 \in (0, S^{in})$ thanks to condition (86). As $\varphi(0, D, r) > 0$ and $\varphi(S^{in}, D, r) < 0$, we deduce the existence of a unique $S_2^\star = S_2^\star(S^{in}, D, r)$ in $(0, S^{in})$ such that $\varphi(S_2^\star, D, r) = 0$, which also verifies $\partial_{S_2}\varphi < 0$ at $S_2 = S_2^\star$.

Then, by the Implicit Function Theorem, the function $(D, r) \mapsto S_2^\star(S^{in}, D, r)$ is C^2 on $\mathcal{D}_\varepsilon$. Recall that for $r < 1$ and $D < r\delta$, on has the expression $G_2(S^{in}, D, r) = VD(S^{in} - S_2^\star(S^{in}, D, r))$ (see Proposition 44). We extend now the function $(D, r) \mapsto G_2(S^{in}, D, r)$ with this last C^2 expression on $\mathcal{D}_\varepsilon$. As $G_2(S^{in}, D, 1) = G_{chem}(S^{in}, D)$ for any $D \in (0, \delta)$, one deduces, by continuity of the partial derivatives of G_2 with respect to D and property (85), the existence of $\mathcal{V}_D$, $\mathcal{V}_r$ as neighborhoods respectively of $\overline{D}(1)$ and 1 with $\mathcal{V}_D \times \mathcal{V}_r \subset \mathcal{D}_\varepsilon$ such that for any $r \in \mathcal{V}_r$, the function $D \mapsto G_2(S^{in}, D, r)$ possesses the following properties

1. it is strictly concave on $\mathcal{V}_D$,

2. it is increasing on $(D_\varepsilon, \overline{D}(1)) \setminus \mathcal{V}_D$ and decreasing on $(\overline{D}(1), r\delta) \setminus \mathcal{V}_D$,

3. its maximum over $(0, r\delta)$ is not reached for $D \leq D_\varepsilon$.

We thus deduce that $D \mapsto G_2(S^{in}, D, r)$ admits a unique maximum $\overline{D}(r)$ on $(0, r\delta)$, for any $r \in \mathcal{V}_r$.

Finally, for any $r \in \mathcal{V}_r$, $\overline{D}(r)$ is characterized as the zero of the map $D \mapsto F(D, r)$ where F is the C^1 function

$$F(D, r) := \partial_D G_2(S^{in}, D, r)$$

From property 1. above, one obtains

$$\partial_D F(\overline{D}(r), r) = \partial_{DD}^2 G_2(S^{in}, \overline{D}(r), r) < 0, \quad r \in \mathcal{V}_r$$

and by the Implicit Function Theorem, there exists a neighborhood $\mathcal{V}_1 \subset \mathcal{V}_r$ of 1 such that $\overline{D}$ is C^1 on $\mathcal{V}_1$, which ends the proof of the lemma.

D.3 Proof of Proposition 6

S^{in} being fixed, we shall drop the S^{in} dependency in the expressions of S_i^*, x_i^* $(i = 1, 2)$ and G_2. Thus, let us define

$$\begin{aligned}
G(D, r) &:= G_2(S^{in}, D, r), \\
F_i(D, r) &:= f(S_i^*(D, r))x_i^*(D, r), \quad i = 1, 2,
\end{aligned}$$

as functions of $D \geq 0$ and $r \in \mathcal{V}_1 \cap \{r < 1\}$. Remark from the expression of F_1, that it is well defined as well as its partial derivatives at $r = 1$. In addition, for the limiting case $r = 1$, using Lemma 9, for all $D \geq 0$, one has

$$\begin{aligned}
S_2^*(D, 1) &= S_1^*(D, 1) = \lambda(D + a) \\
x_2^*(D, 1) &= x_1^*(D, 1) = \frac{D}{D+a}(S^{in} - \lambda(D + a)).
\end{aligned} \tag{87}$$

Thus, for all $D \geq 0$, one has

$$F_1(D, 1) = F_2(D, 1), \tag{88}$$

and F_2 is also well defined for $r = 1$. Thus, according to (37), for all $D \geq 0$ and $r \in \mathcal{V}_1 \cap \{r \leq 1\}$, one has

$$G(D, r) = rF_1(D, r) + (1 - r)F_2(D, r),$$

and from Lemma 4, for $r \in \mathcal{V}_1 \cap \{r < 1\}$, one has

$$\overline{G}(r) = G(\overline{D}(r), r), \tag{89}$$

with $\overline{G}$ defined by (42). For convenience, for a function E of (D, r) that is differentiable, we shall define the three following functions: $\overline{E}(r) := E(\overline{D}(r), r)$ and

$$\partial_r E(r) := \tfrac{\partial E}{\partial r}(\overline{D}(r), r), \quad \partial_D E(r) := \tfrac{\partial E}{\partial D}(\overline{D}(r), r).$$

Therefore, the function $\overline{G}$ writes

$$\overline{G}(r) = r\overline{F}_1(r) + (1-r)\overline{F}_2(r), \text{ for } r \in \mathcal{V}_1 \cap \{r < 1\}. \tag{90}$$

As the functions F_i are differentiable and as $\overline{D}(r)$ is a maximizer of $D \mapsto rF_1(D, r) + (1-r)F_2(D, r)$ on the interior of the interval $[0, f(S^{in}) - a]$, one has

$$r\partial_D F_1(r) + (1-r)\partial_D F_2(r) = 0, \text{ for } r \in \mathcal{V}_1 \cap \{r < 1\}, \tag{91}$$

and $\partial_D F_1(1) = 0$. As f is $\mathcal{C}^2$ and $\overline{D}$ is assumed to be differentiable on $\mathcal{V}_1 \cap \{r < 1\}$, $\overline{G}$ is differentiable and from (90), for all $r \in \mathcal{V}_1 \cap \{r < 1\}$, one has

$$\begin{aligned} \overline{G}'(r) \quad &= \overline{F}_1(r) - \overline{F}_2(r) + r\partial_r F_1(r) + (1-r)\partial_r F_2(r) \\ &\quad + (r\partial_D F_1(r) + (1-r)\partial_D F_2(r))\overline{D}'(r), \end{aligned}$$

and with (91), for all $r \in \mathcal{V}_1 \cap \{r < 1\}$, one has simply

$$\overline{G}'(r) = \overline{F}_1(r) - \overline{F}_2(r) + r\partial_r F_1(r) + (1-r)\partial_r F_2(r). \tag{92}$$

Let us now determine the limits of the terms of the right side of this last equality when r tends to 1. Firstly, according to (88), one has in particular

$$\overline{F}_1(1) = \overline{F}_2(1). \tag{93}$$

Secondly, remark that the dynamics of the first tank is parameterized by the single dilution rate $D_1 = D/r$, the other parameters being fixed (see the expression (66)). The function F_1 takes then the form $F_1(D, r) = \tilde{F}_1(D/r)$ where $\tilde{F}_1$ is a smooth function. Therefore, one has

$$\partial_D F_1(r) = -\frac{r}{\overline{D}(r)} \partial_r F_1(r). \tag{94}$$

As $\partial_D F_1(1) = 0$ then one deduces

$$\partial_r F_1(1) = 0. \tag{95}$$

Finally, from $\dot{S}_2 = 0$, for all $r \in \mathcal{V}_1 \cap \{r < 1\}$, one gets

$$F_2(D, r) = \tfrac{D}{1-r}(S_1^*(D, r) - S_2^*(D, r)). \tag{96}$$

Differentiating (96) with respect to r gives

$$\tfrac{\partial F_2}{\partial r}(D, r) = \tfrac{D}{1-r}\left(\tfrac{\partial S_1^*}{\partial r}(D, r) - \tfrac{\partial S_2^*}{\partial r}(D, r)\right) + \tfrac{D}{(1-r)^2}(S_1^*(D, r) - S_2^*(D, r))$$

which can be written equivalently as

$$(1-r)\tfrac{\partial F_2}{\partial r}(D, r) = D\left(\tfrac{\partial S_1^*}{\partial r}(D, r) - \tfrac{\partial S_2^*}{\partial r}(D, r)\right) + F_2(D, r).$$

Thus, for $D = \overline{D}(r)$, one has

$$(1-r)\partial_r F_2(r) = \overline{D}(r)(\partial_r S_1^*(r) - \partial_r S_2^*(r)) + \overline{F}_2(r).$$

Notice that for $D = \overline{D}(r)$, (96) gives

$$\overline{F}_2(r) = \tfrac{\overline{D}(r)}{1-r}(\overline{S}_1^*(r) - \overline{S}_2^*(r)), \quad \text{for all } r \in \mathcal{V}_1 \cup \{r < 1\}. \tag{97}$$

Using L'Hôpital's rule in (97) when r tends to 1, one gets

$$\overline{F}_2(1) = \lim_{r \to 1^-} \frac{\overline{D}'(r)(\overline{S}_1^*(r) - \overline{S}_2^*(r)) + \overline{D}(r)(\partial_r S_1^*(r) - \partial_r S_2^*(r))}{-1}$$

and using (87) and (93), one obtains

$$\overline{F}_1(1) = \lim_{r \to 1^-} -\overline{D}(r)(\partial_r S_1^*(r) - \partial_r S_2^*(r)).$$

Consequently, one has

$$\lim_{r \to 1^-} (1-r)\partial_r F_2(r) = 0. \tag{98}$$

With (93), (95) and (98), expression (92) gives the existence of the limit of $\overline{G}'$ when r tends to 1 with $r < 1$, which is

$$\overline{G}'(1^-) = 0. \tag{99}$$

Note that $\overline{G}''(1^-)$ exists if and only if $\lim_{r \to 1^-} \frac{\overline{G}'(r) - \overline{G}'(1)}{r-1}$ exists. Using (99) and (92), one has

$$\frac{\overline{G}'(r) - \overline{G}'(1^-)}{r-1} = -\frac{\overline{G}'(r)}{1-r} = -\frac{\overline{F}_1(r) - \overline{F}_2(r) + r\partial_r F_1(r) + (1-r)\partial_r F_2(r)}{1-r} \tag{100}$$

On the one hand, using L'Hôpital's rule, one has

$$\lim_{r \to 1^-} \frac{\overline{F}_1(r) - \overline{F}_2(r)}{1-r} = \lim_{r \to 1^-} \frac{\overline{F}_1'(r) - \overline{F}_2'(r)}{-1}.$$

Recall that $\partial_r F_1(1) = 0$ and thus one has $\overline{F}_1'(1) = 0$. Consequently, one has

$$\lim_{r \to 1^-} \frac{\overline{F}_1(r) - \overline{F}_2(r)}{1-r} = \lim_{r \to 1^-} \overline{F}_2'(r) = \lim_{r \to 1^-} \partial_r F_2(r) + \partial_D F_2(r)\overline{D}'(r). \tag{101}$$

On the other hand, using (91) and (94), one has

$$\frac{r}{1-r}\partial_r F_1(r) = \frac{\overline{D}(r)}{r}\partial_D F_2(r). \tag{102}$$

Thus, according to (100), (101) and (102), one gets

$$\lim_{r \to 1^-} \frac{\overline{G}'(r) - \overline{G}'(1^-)}{r-1} = \lim_{r \to 1^-} -2\partial_r F_2(r) - \left(\frac{\overline{D}(r)}{r} + \overline{D}'(r)\right)\partial_D F_2(r). \tag{103}$$

Let us show now that the limit of $\partial_D F_2(r)$ is 0 when r tends to 1. One has

$$\frac{\partial F_2}{\partial D} = f'(S_2^*)\frac{\partial S_2^*}{\partial D}x_2^* + f(S_2^*)\frac{\partial x_2^*}{\partial D}.$$

Let use the expression $G(D,r) = D(S^{in} - S_2^*(D,r))$ given by Proposition 4. As $\overline{D}(r)$ is a maximizer then one has

$$\partial_D G(r) = S^{in} - \overline{S}_2^*(r) - \overline{D}(r)\partial_D S_2^*(r) = 0.$$

Using (87), one then deduces

$$\partial_D S_2^*(1^-) = \frac{S^{in} - \lambda(\overline{D}(1)+a)}{\overline{D}(1)}.$$

In addition, using expressions (67) and (87), one gets

$$\partial_D x_2^*(1^-) = -\frac{\overline{D}(1)}{(\overline{D}(1)+a)^2}\left(S^{in} - \lambda\left(\overline{D}(1)+a\right)\right),$$

and hence the limit of $\partial_D F_2$ when r tends to 1 exists:

$$\partial_D F_2(1^-) = \frac{S^{in} - \lambda(\overline{D}(1)+a)}{\overline{D}(1)+a}f'\left(\lambda\left(\overline{D}(1)+a\right)\right)A,$$

where $A = S^{in} - \lambda \left(\overline{D}(1) + a \right) - \frac{\overline{D}(1)}{f'\left(\lambda \left(\overline{D}(1) + a \right) \right)}$. Thus, one has

$$\partial_D F_2(1^-) = \frac{S^{in} - \lambda \left(\overline{D}(1) + a \right)}{\overline{D}(1) + a} f' \left(\lambda \left(\overline{D}(r) + a \right) \right) \left(S^{in} - g \left(\overline{D}(1) \right) \right),$$

with g defined by (57). According to Proposition 9, one has $S^{in} - g \left(\overline{D}(1) \right) = 0$. Consequently, one has $\partial_D F_2(1^-) = 0$.

Finally, it remains to calculate the limit of $\partial_r F_2(r)$ when r tends to 1. One has

$$\frac{\partial F_2}{\partial r} = f'(S_2^*) \frac{\partial S_2^*}{\partial r} x_2^* + f(S_2^*) \frac{\partial x_2^*}{\partial r}.$$

Let use again the expression $G(D, r) = D(S^{in} - S_2^*(D, r))$. According to (90), one has

$$\overline{G}'(r) = \partial_r G(r) + \partial_D G(r) \overline{D}'(r)$$

where $\partial_D G(r) = 0$. According to (99), we have $\partial_r G(1^-) = 0$, and thus $\partial_r S_2^*(1^-) = 0$. Using expression (67), one gets

$$\partial_r x_2^*(1^-) = -a \overline{D}(1) \frac{S^{in} - \lambda \left(\overline{D}(1) + a \right)}{\left(\overline{D}(1) + a \right)^2},$$

and then the limit of $\partial_r F_2$ when r tends to 1 exists:

$$\partial_r F_2(1^-) = -a \overline{D}(1) \frac{S^{in} - \lambda \left(\overline{D}(1) + a \right)}{\overline{D}(1) + a}.$$

As $\overline{D}'$ is assumed to be bounded on $\mathcal{V}_1 \cup \{r < 1\}$, we thus obtain from (103) the existence of $\overline{G}''(1^-)$ with

$$\overline{G}''(1^-) = -2 \partial_r F_2(1^-)$$

which is given by expression (43).

References

[1] N. Abdellatif, R. Fekih-Salem and T. Sari, Competition for a single resource and coexistence of several species in the chemostat, Math. Biosci. Eng., 13 (2016), 631–652.

[2] B. Bar and T. Sari, The operating diagram for a model of competition in a chemostat with an external lethal inhibitor, Discrete & Continuous Dyn. Syst. - B, 25 (2020), 2093–2120.

[3] G. Bastin and D. Dochain, On-line estimation and adaptive control of bioreactors: Elsevier, Amsterdam, 1990 (ISBN 0-444-88430-0). xiv+ 379 pp. Price US \$146.25/Dfl. 285.00, Elsevier, (1991).

[4] A. Bornhöft, R. Hanke-Rauschenbach and K. Sundmacher: steady state analysis of the anaerobic digestion model no. 1 (adm1). Nonlinear Dynamics 73 (2013), 535–549. DOI 10.1007/s11071-013-0807-x

[5] M. Crespo and A. Rapaport, About the chemostat model with a lateral diffusive compartment, Journal of Optimization, Theory and Applications, Vol. 185 (2020), 597—621.

[6] M. Dali-Youcef, J. Harmand, A. Rapaport, T. Sari. Some non-intuitive properties of serial chemostats with and without mortality. 2021. https://hal.archives-ouvertes.fr/03404740hal-03404740

[7] M. Dali-Youcef, A. Rapaport and T. Sari, Study of performance criteria of serial configuration of two chemostats, Math. Biosci. Eng., 17(6) (2020), 6278-6309.

[8] M. Dali-Youcef and T. Sari. The productivity of two serial chemostats (2021). https://hal.inrae.fr/hal-03445797

[9] Y. Daoud, N. Abdellatif, T. Sari and J. Harmand: Steady-state analysis of a syntrophic model: The effect of a new input substrate concentration. Math. Model. Nat. Phenom. 13 (2018), 31 . DOI 10.1051/mmnp/2018037

[10] M. Dellal, M. Lakrib and T. Sari, The operating diagram of a model of two competitors in a chemostat with an external inhibitor, Math. Biosci., 302 (2018), 27–45.

[11] R. Fekih-Salem, Y. Daoud, N. Abdellatif and T. Sari. A mathematical model of anaerobic digestion with syntrophic relationship, substrate inhibition and distinct removal rates. *SIAM Journal on Applied Dynamical Systems* 20 (2021), 621–1654.

[12] R. Fekih-Salem, C. Lobry and T. Sari, A density-dependent model of competition for one resource in the chemostat, Math. Biosci., 286 (2017), 104–122.

[13] S. Fogler: Elements of Chemical Reaction Engineering, 4th edition. Prentice Hall, New-York (2008).

[14] C. de Gooijer, W. Bakker, H. Beeftink and J. Tramper, Bioreactors in series: an overview of design procedures and practical applications. Enzyme Microb. Technol. 18 (1996), 202–219.

[15] I. Haidar, A. Rapaport, A. and F. Gérard, Effects of spatial structure and diffusion on the performances of the chemostat. Mathematical Bioscience and Engineering. 8(4) (2011), 953–971.

[16] J. Harmand, C. Lobry, A. Rapaport and T. Sari, The Chemostat: Mathematical Theory of Microorganism Cultures, John Wiley & Sons, Chemical Engineering Series, 2017.

[17] J. Harmand, A. Rapaport and A. Trofino, Optimal design of two interconnected bioreactors–some new results. AIChE J. 49(6) (1999), 1433–1450.

[18] Z. Khedim, B. Benyahia, B. Cherki, T. Sari and J. Harmand: Effect of control parameters on biogas production during the anaerobic digestion of protein-rich substrates. Applied Mathematical Modelling 61 (2018), 351–376 . DOI 1091 10.1016/j.apm.2018.04.020

[19] C.M. Kung and B.C. Baltzis: The growth of pure and simple microbial competitors in a moving and distributed medium. Math. Biosci. 111 (1992), 295–313 .

[20] 0. Levenspiel, Chemical reaction engineering, 3rd edition. Wiley, New York (1999).

[21] B. Li, Global asymptotic behavior of the chemostat : general response functions and differential removal rates. SIAM Journal on Applied Mathematics 59 (1998), 411–4.

[22] R. W. Lovitt and J.W.T. Wimpenny, The gradostat: a tool for investigating microbial growth and interactions in solute gradients. Soc. Gen. Microbial Quart. 6 (1979), 80 .

[23] R. W. Lovitt and J.W.T. Wimpenny, The gradostat: a bidirectional compound chemostat and its applications in microbiological research, *J. Gen. Microbiol.* 127 (1981), 261—268

[24] K. Luyben and J. Tramper, Optimal design for continuously stirred tank reactors in series using Michaelis-Menten kinetics. Biotechnol. Bioeng. 24 (1982), 1217–1220.

[25] M. Nelson and H. Sidhu, Evaluating the performance of a cascade of two bioreactors. Chem. Eng. Sci. 61 (2006), 3159–3166.

[26] S. Pavlou, Computing operating diagrams of bioreactors, J. Biotechnol., 71 (1999), 7–16, 10.1016/s0168-1656(99)00011-5

[27] M. Polihronakis, L. Petrou and A. Deligiannis, Parameter adaptive control techniques for anaerobic digesters—real-life experiments, Elsevier, Computers & chemical engineering, 17(12) (1993), 1167-1179.

[28] A. Rapaport, I. Haidar and J. Harmand, Global dynamics of the buffered chemostat for a general class of growth functions, J. Mathematical Biology, 71(1) (2015), 69–98.

[29] A. Rapaport and J. Harmand, Biological control of the chemostat with nonmonotonic response and different removal rates. Mathematical Biosciences and Engineering 5, no. 3 (2008), 539–547.

[30] T. Sari. Best Operating Conditions for Biogas Production in Some Simple Anaerobic Digestion Models. *Processes* 2022, 10, 258. https://doi.org/10.3390/pr10020258

[31] T. Sari and B. Benyahia. The operating diagram for a two-step anaerobic digestion model. *Nonlinear Dynamics* 2021, **105**, 2711–2737. https://doi.org/10.1007/s11071-021-06722-7

[32] T. Sari and J. Harmand, A model of a syntrophic relationship between two microbial species in a chemostat including maintenance, Math. Biosci., 275 (2016), 1–9.

[33] T. Sari and F. Mazenc, Global dynamics of the chemostat with different removal rates and variable yields. Math Biosci Eng. 8(3) (2011), 827–40.

[34] T. Sari and M.J. Wade, Generalised approach to modelling a three-tiered microbial food-web, Math. Biosci., 291 (2017), 21–37.

[35] M. Sbarciog, M. Loccufier and E. Noldus, Determination of appropriate operating strategies for anaerobic digestion systems, Biochem. Eng. J., 51 (2010), 180–188.

[36] H. Smith, The gradostat: A model of competition along a nutrient gradient. Microbial Ecology, 22(1) (1991), 207–26.

[37] H. Smith, B. Tang and P. Waltman: Competition in a n-vessel gradostat. SIAM J. Appl. Math. 91(5) (1991), 1451–1471.

[38] H. Smith and P. Waltman, The Theory of the Chemostat, Dynamics of Microbial Competition. Cambridge University Press, 1995.

[39] B. Tang, Mathematical investigations of growth of microorganisms in the gradostat, J. Math. Biol., 23 (1986), 319–339.

[40] M.J. Wade, R.W. Pattinson, N.G. Parker and J. Dolfing, Emergent behaviour in a chlorophenol-mineralising three-tiered microbial 'food web', J. Theor. Biol., 389 (2016), 171–186.

[41] M. Weedermann, G. Seo and G.S.K Wolkowics: Mathematical model of anaerobic digestion in a chemostat: Effects of syntrophy and inhibition. Journal of Biological Dynamics 7 (2013), 59–85. DOI 10.1080/17513758.2012.755573

[42] M. Weedermann, G.S.K Wolkowicz and J. Sasara: Optimal biogas production in a model for anaerobic digestion. Nonlinear Dynamics 81 (2015), 1097–1112.

[43] G.S.K. Wolkowicz, Z. Lu,Global dynamics of a mathematical model of competition in the chemostat: general response functions and differential death rates. SIAM Journal on Applied Mathematics 52 (1992), 222–23.

[44] A. Xu, J. Dolfing, T.P. Curtis, G. Montague and E. Martin, Maintenance affects the stability of a two-tiered microbial 'food chain'?, J. Theor. Biol., 276 (2011), 35–41.

[45] J. Zambrano, B. Carlsson and S. Diehl, Optimal steady-state design of zone volumes of bioreactors with Monod growth kinetics. Biochem. Eng. J. 100 (2015), 59–66.